2014

LIPOSOMES FOR THE CONTROLLED DELIVERY OF MULTIPLE DRUGS

Swapnil A. Malekar
University of Rhode Island, swapnil2284@gmail.com

LIPOSOMES FOR THE CONTROLLED DELIVERY OF MULTIPLE DRUGS

BY

SWAPNIL A. MALEKAR

A DISSERTATION SUBMITTED IN PARTIAL FULFILLMENT OF THE

REQUIREMENTS FOR THE DEGREE OF

DOCTOR OF PHILOSOPHY

IN

PHARMACEUTICAL SCIENCES

COLLEGE OF PHARMACY

UNIVERSITY OF RHODE ISLAND

2014

DOCTOR OF PHILOSOPHY DISSERTATION

OF

SWAPNIL A. MALEKAR

APPROVED:

Thesis Committee:

Major Professor David R. Worthen

Navindra Seeram

Arijit Bose

Nasser H. Zawia
DEAN OF THE GRADUATE SCHOOL

UNIVERSITY OF RHODE ISLAND
2014

ABSTRACT

Various pathological conditions, such as cancer, osteoporosis, AIDS, tuberculosis, and other pathologies, require the concurrent use of multiple drugs, known as combination therapy or polytherapy, for effective treatment. The concurrent delivery of multiple drugs in a single dosage form, such as a tablet, capsule or parenteral, has been demonstrated in a number of products, but current technologies for multiple drug delivery remain limited for broad application. Physicochemical incompatibility, limited aqueous and lipid solubility, and chemical instability of the individual drugs, as well as detrimental drug-drug and drug-excipient interactions within the multiple-component dosage form, may all compromise the development of stable, multiple drug delivery systems.

Liposomes have been employed for the delivery of pharmaceuticals, nutraceuticals, and cosmetics for a number of years. Liposomes are now emerging as potential tools for the delivery of multiple therapeutic and diagnostic agents in a single dosage form. While useful for some pharmaceutical applications, liposomes may have certain limitations, such as low drug encapsulation efficiency, poor mechanical and physical stability, and fragile structures that can lead to premature release of encapsulated drug before reaching the target site. Empirical attempts have been made to assemble liposomal structures and divide the space controllably and spontaneously at a nanometer scale into hydrophobic and hydrophilic regions. By understanding the nature of the different microenvironments located within liposomes, multiple drugs with a wide range of physiochemical properties may be incorporated into appropriately designed liposomal structures. Various modifications can be made to the

composition and surface modification of liposomes in order to control their size, enhance their stability, and incorporate a combination of multiple therapeutic and diagnostic agents, thereby producing a polyfunctional 'theranostic' liposome for improved therapeutic compliance and clinical effectiveness.

We hypothesize that in order make these liposomes and optimize the drug delivery it is necessary to understand the liposome formation procedure with emphasis on the nature of both aqueous and lipid microenvironments so that suitable combinations of therapeutics and diagnostics can be identified and incorporated into the liposome system. Optimization of these nanostructures is necessary in order to enhance their stability while emphasizing the use of GRAS (generally regarded as safe) materials and conforming to compendial standards for injectables. This is followed by characterization of these delivery devices in terms of their structure, drug loading, size, morphology, thermal characteristics, reproducibility of formulation, and stability using microscopic, light, electric, magnetic, chromatographic, and thermal analysis, as well as an appreciation of the interaction of encapsulated small molecules with lipid components. Finally, an evaluation of the performance of these vesicles as controlled delivery devices using an externally applied magnetic field in order to trigger bolus or pulsatile drug release is summarized.

This study has provided important predictive information regarding the formation, formulation, stability, and performance characteristics of theranostic liposomal delivery systems in the context of the specific physicochemical properties of selected combinations of chemically diverse drugs and other small molecules that are nevertheless clinically relevant. It is hypothesized that these data will be useful in the

design and optimization of analogous systems containing drugs with similar properties. The use of a magnetic field-induced release mechanism will afford data regarding the utility of this controlled release mechanism in multiple drug-containing systems. The successful design and characterization of these systems may lead to improved therapeutic efficacy of combination drug therapy, increased patient compliance, ease of use, and targeted drug delivery for reducing both dosing frequency and toxicity.

The work has been prepared for publication and included in the thesis as follows:

1) Manuscript 1: Design and development of liposomes for concurrent, controlled delivery of therapeutic agents for bone osteoporosis (in preparation ***Pharmaceutical Research***).

2) Manuscript 2: The interactions and effects of di- and polyphenolic compounds on lipid vesicles (in preparation ***Lipid Research***).

3) Manuscript 3: The design and development of liposomes for the concurrent, controlled delivery of multiple therapeutic agents for improving the efficacy of pancreatic cancer treatment (in preparation ***Journal of Controlled Release***).

Manuscript 1: Radiofrequency-activated nano liposomes for controlled multi-drug delivery.

This manuscript focuses on the use of a hydrophilic tetracycline antibiotic, doxycycline HCl, and a hydrophobic, estrogenic anti-osteoporosis drug, raloxifene HCl, and their incorporation into liposomes. These drugs are incorporated into the different aqueous and lipid microenvironments of the liposome. The delivery of these

drugs is controlled by using hydrophobic iron oxide nanoparticles that are coated with oleic acid. Given the disparate physicochemical characteristics of the two drugs, there were some untoward compatibility and stability issues that arose. These instabilities were addressed by optimizing the drug concentrations and integrating block copolymers in order to sterically stabilize the liposomes.

In-depth analyses and characterization of these delivery devices, including size, morphology, reproducible formulation, drug loading and release, and stability, followed by their optimization for drug delivery in compliance with the compendial standards and *in vitro* release patterns, were also performed.

Since the drugs have different physiochemical properties, their interactions with the liposomal bilayers were different. These interactions were carefully analyzed using various light, magnetic, electric and thermal techniques and, where appropriate, NMR spectrometry. The rate and extent of drug release from these liposome constructs, with and without magnetic nanoparticle-induced drug release, was studied in a physiologically relevant media (137 mM phosphate buffered saline, pH 7.4). During this study, we observed that raloxifene HCl (a di- phenolic, hydrophobic drug) had a pronounced effect on the transition temperature of liposomes that led to the investigation of the effect of various other lipophilic, di- and polyphenolic compounds, on liposomes. This work is shown in the following manuscript.

Manuscript 2: The interactions and effects of di- and polyphenolic compounds on lipid vesicles.

This study focuses on the interactions of various hydrophobic, di- and polyphenolic drugs and nutraceuticals, including raloxifene, garcinol, resveratrol, quercetin and bisphenol A, with DPPC liposomes. These drugs and nutritional compounds belong to BCS classes II and IV. As such, they all have very low aqueous solubility, which would suggest a tendency to be incorporated into the hydrophobic bilayers. In addition, the BCS Class IV compounds also have very low tissue permeability. Due to the likely interaction of these agents with the vesicular lipid bilayers, they were capable of changing the thermodynamic properties, packing parameter, and stability of these bilayers. These changes in the liposomal properties was characterized by studying their zeta potential, particle size as a function of time, nano Differential Scanning Calorimetry (nano-DSC), ^{1}H-NMR (proton nuclear magnetic resonance) and ^{31}P-NMR (phosphorus nuclear magnetic resonance) spectrometry. It was hypothesized that these phenolic compounds may interact with the phosphate head groups and/or the acyl chains of the DPPC and thereby increase the transition temperature of DPPC bilayers. With an increase in the transition temperature, the liposomes were expected to become more thermodynamically stable, as a greater amount of energy would be required to convert them from the rippled gel to the liquid crystalline phase. Any increased exposure of the phosphate groups to the external suspension media induced by polyphenolic interactions might lead to an increase in the negative surface charge, as determined by zeta potential measurements. This increased surface charge can lead to repulsive forces between the liposomes and

might further enhance liposome stability. The overall effect of polyphenolics on DPPC liposomes, if favorable, might be utilized to form stable liposomes characterized by minimal drug leakage, which is a common disadvantage of liposomal drug delivery systems, as well as lead to extended shelf life and improved handling on shipping and storage.

Manuscript 3: The design and development of liposomes for the controlled delivery of multiple therapeutic drugs for pancreatic cancer.

In this study, liposomes comprising 1, 2-Dipalmitoyl-sn-glycero-3-phospocholine monohydrate (DPPC) were used to encapsulate a combination of chemosensitizing, chemotherapeutic, and tumor resistance modulating agents, namely gemcitabine and the COX-2 (cyclooxygenase 2) inhibitor celecoxib. The liposomes were first loaded with each individual drug and then characterized with various light, magnetic, electrical, and thermal techniques. There was a difference in the release pattern of the drugs, perhaps due to differences in their physiochemical properties and likely disparate interactions with the bilayers and solubility in the aqueous core. After evaluating the single-drug containing liposomes, analogous characterization and evaluation of the performance of the liposomes containing combinations of the active agents were conducted. The stabilized liposomes that had uniform particle sizes loaded with both the drugs and magnetic nano particles were incubated for 48 hours with BxPc-3 human pancreatic cancer cells. Cell viability was then determined by performing an MTT assay. In order to assess the utility of magnetic nanoparticle-induced drug release in this in vitro system, analogous experiments were carried out

using one or more representative liposome system with and without magnetic nanoparticles. The results were compared to those obtained from analogous experiments assessing the cytotoxicity of combinations of free drug. It was found that the liposomal formulations containing drug combinations induced maximum cell death, as the chemosensitizers likely increased the sensitivity of the BxPc-3 cell lines towards gemcitabine.

ACKNOWLEDGMENTS

This doctoral dissertation is a product of culmination of my avid interest in Pharmaceutical Sciences for over a decade. The path so far has been very challenging and pleasantly memorable at the same time. There are a lot of people in my life, without whom, it would not have been possible for me to go through all these years.

Above all, I would like to express my gratitude to my major advisor, **Dr. David R. Worthen**. He has supported me not just scientifically but also morally. I knew that I wanted to work for him the day I first met him four years ago. He is the funniest and smartest person I know. I can only wish to be as enthusiastic and energetic as him, someone who never fails to impress people. Apart from helping me continuously with my research, Dr. Worthen also allowed me to concurrently pursue my MBA, which I should be finishing up very soon. I will be in his debt for my entire life for always having faith in me. No matter how stressed I was due to my PhD research, TA duties, MBA, or day-to-day activities, his motivational speeches and continuous reference to perseverance gave me the energy to get through the day.

I would also like to thank **Dr. Ashish L. Sarode** for his immense scientific input and discussions, especially when I did not know how to proceed with a particular experiment. His industry experience and due diligence was always of vital importance in the functioning of lab. Just like on the cricket field, his instruction in the lab has led to very fruitful results.

I had never thought that I would be dealing with NMR in my life because the NMR room itself was very intimidating in the first place. I will be forever thankful to **Dr. Alvin C. Bach II** for walking me step-by-step through the instrumentation and data analysis of NMR. His words- "we do not give away these diplomas just for showing up"- always kept me going.

I would like to thank **Dr. Richard Kingsley** for his help with the TEM and EDS instrument. Despite a very busy schedule, he would always find time to run my samples and had the backup of all my files when the main computer had crashed. I still remember the big smile on my face when I discovered that I did not had to repeat the experiments.

I would also like to thank **Dr. Geoffrey Bothun** and **Dr. Arijit Bose** for giving me continuous feedback on my data. Their vast experience and immense knowledge in the field of liposomes and colloidal systems, has helped me a lot in taking my research to the next level.

Finally I would like to extend my sincere thanks to my committee members **Dr. Navindra Seeram** and **Dr. Wei Lu**.

I am thankful to the **College of Pharmacy**, University of Rhode Island for giving me this research opportunity and financially supporting me with teaching assistantships for four years.

I would like to dedicate this work to my mother, **Sandhya Malekar**, for being a constant support and a source of inspiration throughout my life. It would not have been possible for me to achieve all that I have today without her encouragement and valuable advice. As T. DeWitt Talmage said, she was the bank where I deposited all my hurts and worries. I am grateful to my late father, my hero and my role model, **Mr. A. G. Malekar,** for giving me the opportunity to pursue my dream of higher education in the US. There is not a single day that goes by when I don't miss him. I would also like to thank my younger brother, **Nikhil Malekar,** for his moral support, patience and showing faith in me.

There are too many friends to thank here (you all know who you are) for always being there when I needed you the most.

PREFACE

This dissertation was prepared according to the University of Rhode Island "Guidelines for the format of Thesis and Dissertations" standards for manuscript format. This dissertation comprises of three manuscripts that have been assembled in order to satisfy the requirements of the Department of Biomedical and Pharmaceutical Sciences, College of Pharmacy, University of Rhode Island.

Manuscript 1: Radiofrequency-activated nano liposomes for controlled multi-drug delivery.

This manuscript is being prepared for submission to ***Pharmaceutical Research***.

Manuscript 2: The interactions and effects of di- and polyphenolic compounds on lipid vesicles.

This manuscript is being prepared for submission to ***Lipid Research***.

Manuscript 3: Design and development of liposomes for the controlled delivery of multiple therapeutic drugs for pancreatic cancer.

This manuscript is being prepared for submission in ***Journal of Controlled Release***.

TABLE OF CONTENTS

LIST OF TABLES

LIST OF FIGURES

Chapter 3

Chapter 1:

This manuscript is being prepared for submission to ***Pharmaceutical Research***.

Radiofrequency-activated nano liposomes for controlled multi-drug delivery.

Swapnil A. Malekar[1], Ashish L. Sarode[1], Alvin C. Bach II[1], Arijit Bose[2], Geoffrey Bothun[2], and David R. Worthen[1, 2*]

[1]Department of Biomedical and Pharmaceutical Sciences, College of Pharmacy and [2]Department of Chemical Engineering, College of Engineering, University of Rhode Island, Kingston, RI 02881

*Author to whom correspondence should be addressed:

495M Pharmacy Building,

7 Greenhouse Drive,

University of Rhode Island,

Kingston, RI 02881

Tel. 401-874-5016

email: dworthen@ds.uri.edu

ABSTRACT

An important goal in therapeutics is the delivery of multiple drugs via delivery vehicles that are stable, but release their payload through a triggering mechanism. As an example of such a multifunctional vehicle, we have produced poloxamer stabilized DPPC-based nano liposomes containing doxycycline HCl (DOX), raloxifene HCl (RAL) and magnetic nano particles (MNP's) in the membrane wall. We observed minimal release of the encapsulated drugs until electromagnetic radiation at RF frequencies was applied. RAL had a pronounced stabilizing effect on the liposomes and the release of DOX from the MNP containing liposomes was evident after radiation. Using a range of analytical tools, we show how intermolecular interactions are key to the stability and release of encapsulants from these vehicles. These studies give important insight into the design and optimization of multi-drug containing delivery vehicles for advanced therapeutic applications.

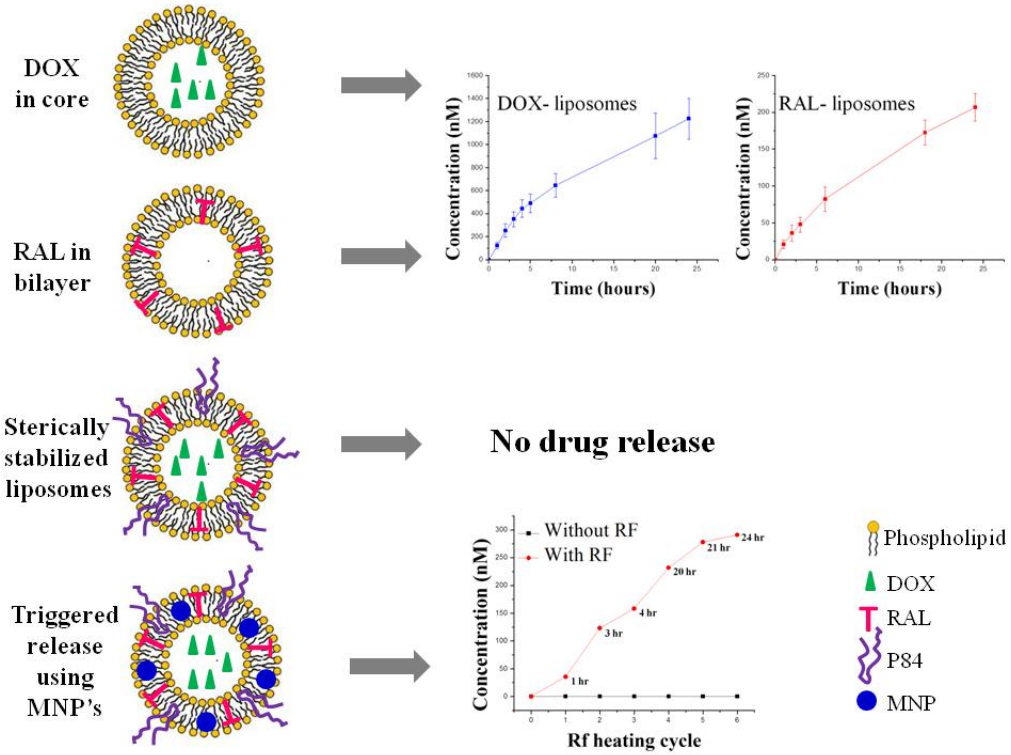

1. INTRODUCTION

Liposomes and other lipid-based vesicular systems have been investigated for over 40 years as drug delivery systems for various therapeutic agents, such as anticancer, antifungal, analgesic, gene therapy, and other active pharmaceutical ingredients.[1] Liposomes are versatile candidates for the delivery of multiple cargos, as their interfacial and surface properties can be easily modified.[2] The hydrophilic components can be dissolved in the aqueous cores of the liposomes while the hydrophobic compounds can be incorporated into the bilayers.[3] However, the stability of liposomes is always a major concern,[4] leading to liposomal cargo leakage, and thus a decline in the availability of the drugs at specific sites.

Various attempts have been made in the past to stabilize liposomes, such as the inclusion of cholesterol in order to increase the bilayer rigidity, using phospholipids of high transition temperatures, polymerization of modified lipids, freeze-thawing and the insertion of block copolymers.[5-7] Furthermore, the stability of liposomes can also be achieved by steric hindrance with the aid of poloxamer block co-polymers known as Pluronics® (PL).[8] By using various grades of PL's that differ in their respective hydrophilic (PEO) and hydrophobic (PPO) blocks, liposomes can be stabilized.[9] With the inclusion of PL's during thin film formation procedure, i.e., dissolving it in the organic solvent along with the lipid, the mechanism of desorption or "squeezing out" can be prevented which might be the case if they were added after liposomes were formed. Thus, PL's can become an integral part of the vesicles and aid in their stability for an enhanced period of time.[10, 11]

Since the release of hydrophilic drugs encapsulated in the liposomal core is driven by passive diffusion, the insertion of PPO chains into the bilayers hinders this transport.[12] An enhanced rigidity of the bilayer imparted by the inclusion of hydrophobic drugs may further reduce this release rate. Moreover, release of hydrophobic compounds embedded within the bilayer can be challenging due to the strong hydrophobic interactions between the drugs and the lipid chains. A high frequency AC magnetic field has been reported to trigger the drug release from liposomes and polymersomes with the use of super paramagnetic iron oxide nano particles (SPIO).[13,14] These SPIO's are biocompatible with minimal *in vivo* toxicity and have also been used as diagnostic agents.[15]

In this investigation we report the formulation of multiple drugs using sterically stabilized liposomes with the aid of a triblock copolymer and the concurrent use of radio frequency magnetic fields with an aim to trigger the release of encapsulated hydrophilic drug. A highly water soluble BCS Class I drug, doxycycline hydrochloride (DOX) was used as a model drug and encapsulated into the hydrophilic cores of the liposomes, whereas a poorly water soluble model drug raloxifene hydrochloride (RAL) was incorporated into the liposome bilayer. The liposomes were stabilized using triblock copolymers pluronics and a triggered release was obtained by incorporating SPIO into the liposome bilayer using a high frequency AC magnetic field.

2. MATERIALS AND METHODS

2.1. Materials. 1, 2-Dipalmitoyl-sn-glycero-3-phospocholine monohydrate (DPPC) was purchased from Corden Pharma (Colorado, USA). Doxycycline hydrochloride (DOX) and raloxifene hydrochloride (RAL) were purchased from Fisher Scientific (Pittsburgh, PA). All Pluronic polymers were purchased from BASF (Parsippany, NJ). Cellulose membranes (Spectra/Por MW cutoff 3500 Da), used for dialysis and drug release tests, were obtained from Spectrum Laboratories, Inc. (Houston, TX). Phosphate buffered saline (PBS) tablets were purchased from MP Biomedicals (Solon, OH). SPIO maghemite nanoparticles (5 nm, 24 mg ml^{-1} or 187.9 mM Fe_2O_3) dispersed in chloroform were purchased from Ocean Nanotech (Springdale, AR). On the basis of the density of maghemite (4.9 g cm^{-3}), 24 mg ml^{-1} is equivalent to 1.43×10^{17} particles ml^{-1}. All other reagents were purchased from Fisher Scientific and were of analytical grade.

2.2. Liposome preparation. Vesicles were prepared at a 17 mM lipid concentration for all formulations. For the ^{31}P-NMR, the vesicles were made in 90:10 (water: D_2O). The vesicles were prepared in 4 ml batches by film rehydration (3 ml for dialysis and drug release studies and 1 ml for characterization) as described by Chen *et al*.[16] The samples were further diluted to a lipid concentration of 5.6 mM for TEM, 1 mM for DLS and zeta potential, and 0.1 mM for nano-DSC. When individual drugs were loaded in liposomes, their final concentration was maintained at 2 mM. When the two-drug combination was encapsulated, their concentrations were reduced to 0.5 mM, as higher two-drug concentrations resulted in vesicular aggregation and instability. The

procedure was same for all the formulations except for the step in which various components were added differed for different formulations. DOX- containing liposomes were prepared by dissolving 50 mg of DPPC in 4 ml of chloroform. Chloroform was removed by rotary evaporation at 50 °C (above the DPPC melting temperature) starting at 450 mbar for 30 min, then decreased to 300 mbar for 30 min, and finally 200 mbar for 30 min. This lipid film was kept under vacuum for 2 hours at room temperature to remove traces of chloroform. It was then rehydrated with a 2 mM DOX in 137 mM PBS for 2 hours at 50 °C. RAL liposomes were analogously prepared. RAL and DPPC were dissolved in a 3:1 ratio of chloroform: methanol due to the insolubility of RAL in pure chloroform. The organic solvents were removed by rotary evaporation at 50 °C (above the DPPC melting temperature) starting at 450 mbar for 30 min, then decreased to 300 mbar for 30 min, and finally 200 mbar for 30 min. This lipid film was kept under vacuum for 2 hours at room temperature to remove traces of organic solvents. The film was rehydrated with 137 mM PBS and the final RAL concentration in the formulation was 2 mM. The magnetic nano-particles (MNP's), RAL, DOX and Pluronic® P84 (P84) containing liposomes were prepared in a similar way by adding the MNP's [lipid/MNP (L/N) ratios of 5000:1, 10000:1 and 20000:1] and P84 to the organic solvent mixture containing lipid and RAL and following the film formation as described above using rotary evaporator and rehydrating the film with 0.5 mM DOX in 137 mM PBS. The resulting aqueous dispersions were then sonicated for 1 hr using a bath sonicator.

2.3. Cryogenic Transmission Electron Microscopy (Cryo-TEM). Cryo-TEM samples were prepared at 25 °C using a Vitrobot (FEI Company), which is a PC-controlled robot for sample vitrification. Quantifoil grids were used with 2 μm carbon holes on 200 square mesh copper grids (Electron Microscopy Sciences, Hatfield, PA). Samples were first equilibrated within the Vitrobot at 25 °C and 100% humidity for 30 min. After immersing the grid into the sample, it was then removed, blotted to reduce film thickness, and vitrified in liquid ethane. The sample was then transferred to liquid nitrogen for storage. Imaging was performed in a cooled microscopy stage (Model 915, Gatan Inc., Pleasanton, CA) at 200 kV using a JEOL JEM-2100F TEM (Peabody, MA).

2.4. Energy dispersive X-ray scattering (EDS). EDS (Model INCAx-act, Oxford Instrument, K) was used to detect elemental iron from the magnetic nanoparticles within the iron oxide nanoparticle-loaded liposomes. EDS was conducted during cryogenic imaging with 158 s of live time and 92 s of dead time.

2.5. ^{31}Phosphorus- Nuclear Magnetic Resonance (^{31}P-NMR). The ^{31}P-NMR spectra were acquired on an Agilent NMRS 500 NMR spectrometer operating at 202.3 MHz using a 5mm NMRone probe. The probe temperature was thermostated at 37 °C for all experiments. Liposome formulations analyzed by NMR were prepared as previously described with the exception that 10% D_2O in water was used as a solvent in order to provide a deuterium lock signal. NMR data were collected for 60 K scans with a 35.7 kHz sweep width using 131 K data points. Acquisition time was 1.3 sec with a

relaxation delay of 0.5 sec. The data were processed with mnova program V8.1 Mesterlab research SL. A line broadening of 50 Hz was applied to all spectra. All spectra were indirectly referenced to H_3PO_4 set to 0 ppm. Data were acquired without spinning.

2.6. Nano Differential Scanning Calorimetry (nano-DSC). Nano-DSC was performed using a TA Instruments Nano DSC (New Castle, DE, USA). Samples at a concentration of 0.1 mM lipid were degassed under vacuum for 30 min before loading into a 0.6 mL capillary cell. The cell was then pressurized with nitrogen to 1 atm and equilibrated at 25 °C. The sample was scanned at 1 °C min^{-1} over a range of 25 °C to 60 °C.

2.7. High Performance Liquid Chromatography (For quantification of dissolution). The HPLC system comprised a Hitachi La Chrome Elite equipped with a PDA detector and an automatic injector with a loop volume of 0.1 ml. For DOX quantification, an Agilent Zorbax SB C8 (5 micron, 4.6 x 250 mm) column was used. The mobile phase consisted of 0.02 M oxalic acid/ methanol/ acetonitrile (65/25/10) with a final pH of 2.5. The flow rate was 1 ml min^{-1} with an injection volume of 90 µl and a detection wavelength of 350 nm. The limit of detection of DOX using this method was 20 nM. The calibration curve in PBS was $R^2 = 0.999$. The column used for RAL quantification was a Luna 3 micron C18 (2) 150 x 4.6 mm with a mobile phase comprising 0.05 M ammonium acetate/ acetonitrile (67/33) with a final pH of 4.0. The flow rate was 1 ml min^{-1} with an injection volume of 90 µl and a detection

wavelength of 287 nm. The limit of detection was 20 nM and the calibration curve in PBS was $R^2 = 0.9997$. The R^2 linearity gives a correlation between the concentration of drug and the area under the curve of the HPLC chromatogram. R^2 value of 0.999 over a range of 20 nM to 200,000 nM suggests accurate quantification of drug derived from corresponding HPLC chromatograms.

2.8. Dynamic Light Scattering. DLS measurements were performed using a Malvern Instruments Zetasizer Nano ZS with a backscattering detector angle of 173° and a 4 mW, 633 nm He-Ne laser (Worcestershire, UK). For size distribution studies, 1 ml of the liposome formulations was analyzed in an optical grade polystyrene cuvette at 37 °C. Before analysis, the samples were stored at 37 °C and then analyzed after 24 hours.

2.9. Radio frequency (RF)-induced drug release. Drug-loaded liposomes containing magnetic nanoparticles were placed in a copper heating coil (3 turns at 4.5 cm mean diameter) around a custom-designed polycarbonate container with a holder for SpectraPor dialysis tubing. Heating was conducted as a function of time and electromagnetic field strength using a 1 kW Hotshot (Ameritherm Inc., Scottsville, NY) operating up to 250 A and 281 kHz. Samples were collected from the drug dissolution media at serial time points during the drug release experiments, and drug concentrations as a function of time were then determined using HPLC.

2.10. Dialysis and Release studies. The dialysis experiment were conducted at room temperature (25 ± 0.5 °C) using 3.5 kDa tubular cellulose acetate membranes for 24 hours in 137 mM PBS with constant stirring and replacement of the dissolution media. The dissolution media was collected and analyzed by HPLC for unencapsulated drug in order to calculate the drug loading capacity of the liposomes. Drug release studies were performed using the same dialysis tubing. The experiments were carried out in 137 mM PBS at 37 ± 0.5 °C and a pH of 7.4 with a stirring speed of 75 rpm using a 0.5 inch magnetic stirrer. Fresh media was replaced after the sampling was done at regular time intervals.

3. RESULTS AND DISCUSSION

3.1 Morphological characterization of the vesicles. It is essential to interpret the structural characteristics of the liposomes such as their size and shape with the incorporation of P84, MNPs, DOX and RAL. Hence, in order to study the morphological characteristics and incorporation of MNPs into the bilayer, Cryo-TEM and EDS analysis of the liposomes was performed. The morphological characteristics of liposomal formulations at 2 mM individual drug concentrations are shown in Figure 1 (a, b).

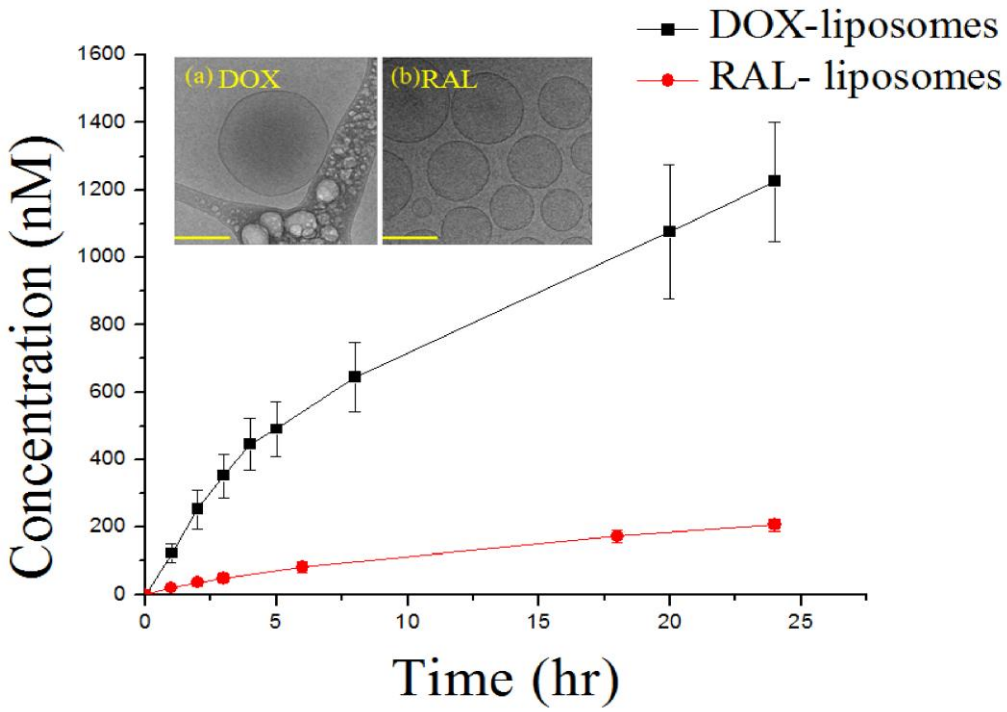

Figure 1. DOX and RAL release from DPPC liposomes carried out at 37 °C and pH 7.4 in 137 mM PBS. 1.88 mM of DOX and 1.98 mM RAL was encapsulated after 20 hours of dialysis which corresponds to encapsulation efficiency of 94.5% and 99.3% respectively. Cryo-TEM images of corresponding (a) DOX and (b) RAL containing liposomes indicating no difference in the morphology. Scale bar is 200nm for the TEM images.

Both DOX- and RAL-containing liposomes were similar in shape with a bilayer thickness of 5 nm, suggesting that the drugs alone did not influence liposomal morphology. The formulations containing both P84 and MNP's were also analyzed for their morphology and elemental composition (Figure 2).

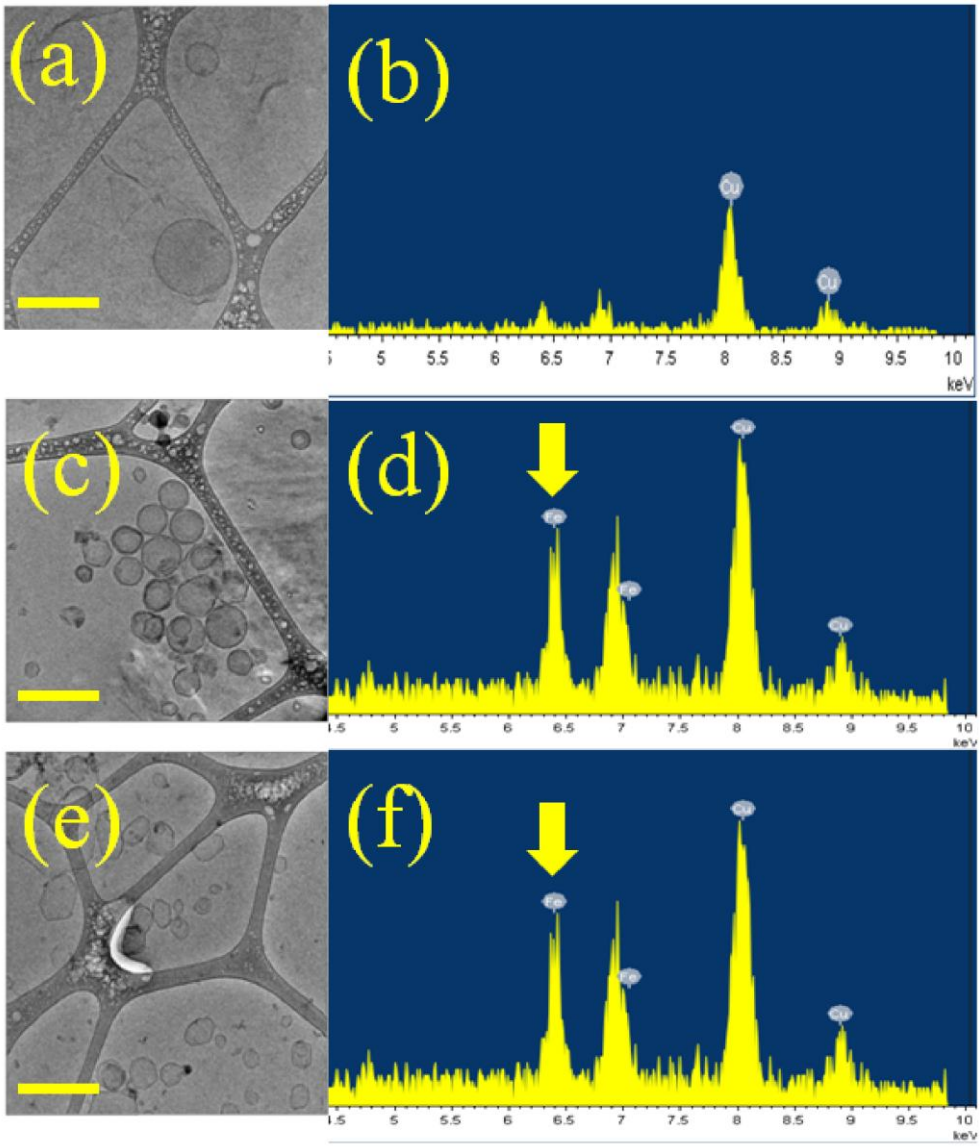

Figure 2. Cryo- TEM images (a) and EDS scans (b) of liposomes containing DOX, RAL and P84 which shows absence of iron peak at 6.4 keV. Cryo-TEM images and EDS scans of liposomes containing DOX, RAL, P84 and MNP's before (c, d) and after (e, f) RF exposure. The L/N ratio was 10000:1 for these formulations. Yellow arrows indicate the presence of MNP's in the bilayers. The round shape of liposomes was converted to angular showing the influence of RF heating on the bilayers. Scale bar is 200nm.

Formulations that did not contain MNP's did not show any iron peak. Formulations containing MNP's depicted distinct iron peaks at 6.4 KeV (indicated with yellow arrows). There was no evidence of the presence of MNP's or aggregates of MNP's outside of the liposomes, suggesting that the MNP's were successfully incorporated into the lipid bilayers as previously reported.[16] The EDS scans were taken in the specific areas of the grid that had liposomes and no prevalent iron oxide nano particles. Thus, it is proved that iron oxide nano-particles were successfully incorporated into the bilayers that triggered the cargo release by using external magnetic field.

3.2. Stability of liposomes. Polydispersity index (PDI) was obtained from photon correlation spectroscopic analysis, giving a dimensionless number extrapolated from the autocorrelation function. Samples with very broad size distribution have polydispersity index values > 0.7. The PDI of all liposome formulations assessed in the present study was detected below 0.3 suggesting a small particle size distribution and homogenous liposomal formulations. The liposomal formulations were further characterized by DLS at various time points to estimate the stability at physiological temperature (Figure 3).

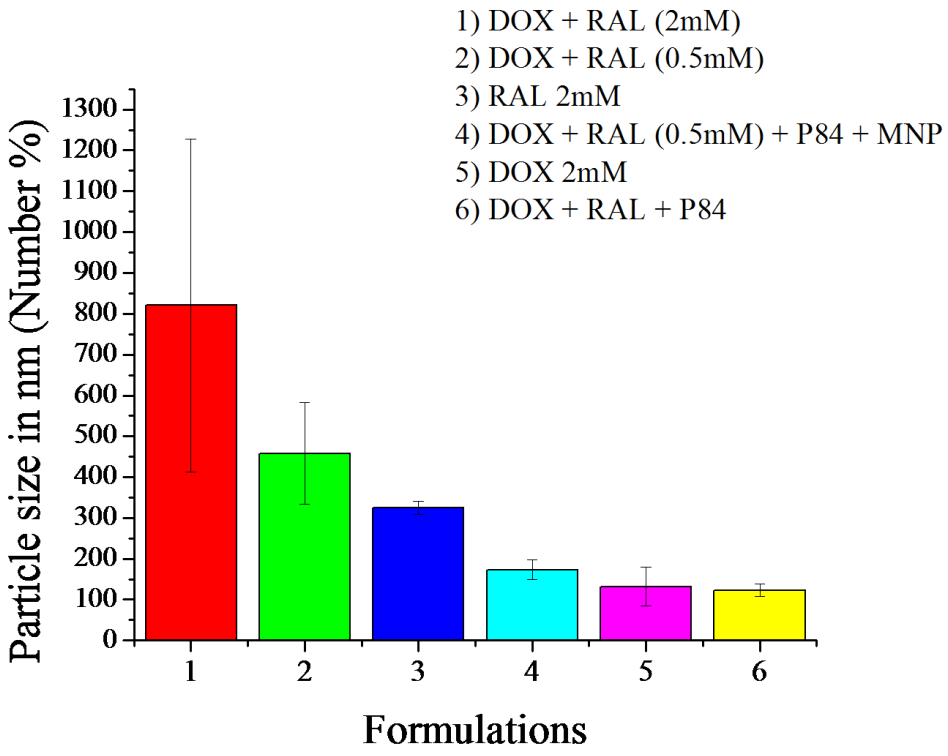

Figure 3. Hydrodynamic diameter of liposomal formulations indicating stability attained by P84.

By taking into consideration the goal of multiple drug loading, when 2 mM of both DOX and RAL were loaded into analogous liposomal systems, large aggregates formed within a couple of hours, perhaps because of the adsorbed DOX. In order to prepare stable liposomes containing both drugs, their concentration was reduced from 2 mM to 0.5 mM each considering this limitation of colloidal stability maybe due to DOX adsorption. The reduction in drug concentration did not improve the stability and since we aimed to make stabilized nano liposomes, poly (ethylene oxide)-poly (propylene oxide)-poly (ethylene oxide) triblock copolymers, or generally known as poloxamers such as Pluronics® (PL) were added to the bilayers to enhance vesicular stability.[8] Pluronics® F-127 and F-108 are proven to increase the mechanical stability

of lipid based vesicular systems, such as dioleoylphosphatidylethanolamine liposomes.[17] Therefore, various grades of PL's were incorporated at different weight percent into the liposomal bilayers in order to stabilize the liposomes containing 0.5 mM of both DOX and RAL respectively (Table 1).

Pluronic grade	**Monomer ratio**
F108	PEO_{132}-PPO_{50}-PEO_{132}
F68	PEO_{76}-PPO_{30}-PEO_{76}
F127	PEO_{100}-PPO_{65}-PEO_{100}
P84	PEO_{19}-PPO_{39}-PEO_{19}

Table 1. Various grades of Pluronics used to stabilize the liposomes along with the individual monomer ratios of PEO: PPO.

Among the four grades of PL that were assessed as liposome stabilizers, only P84 enhanced vesicular stability. Since P84 has the lowest hydrophilic / hydrophobic (PEO/ PPO) ratio, the hydrophobic PPO chains of this particular polymer grade might undergo the most pronounced insertion into the hydrophobic bilayers of the liposomes, resulting in mechanical stabilization. With the increase in the hydrophilic moiety of the copolymer PEO, there is a possibility of "squeezing out" of the copolymer from the lipid bilayers. With P84 at 1:10 (PL:DPPC) w/w ratio, the optimum amount of

hydrophilic PEO chains on the surface and PPO chains inserted into the bilayers of each liposome likely improved vesicular stability due to steric hindrance.[18]

3.3. Characterization of the bilayer. The change in the transition temperature of a vesicular lipid bilayer depends on the presence of other chemical species and their subsequent interaction within the different domains of the vesicles. The interactions of DOX, RAL and combinations thereof were thermally analyzed with nano DSC (Figure 4).

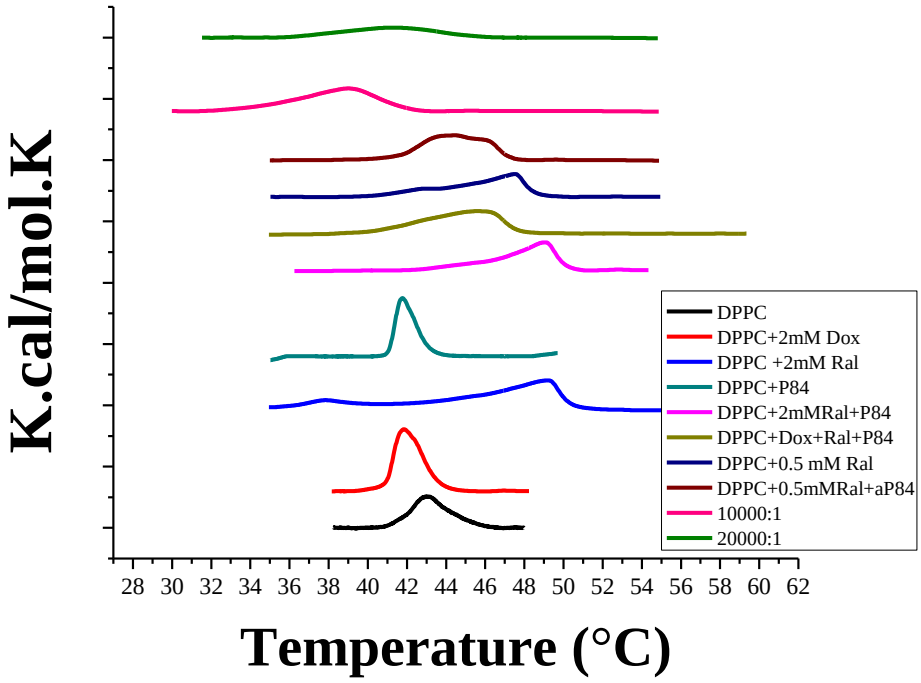

Figure 4. Nano DSC thermographs of the liposomal formulations. RAL increased the T_m of the liposomal bilayer, whereas the T_m was reduced using MNPs and peak broadening was observed with P84. DOX and P84 did not have any effect on the T_m.

Formulations	**ΔH**	**ΔS**	**T_m**
	(Kcal/mol)	**[Kcal/(mol.K)]**	**(°C)**
Blank DPPC	8.43	0.1963	42.96
DPPC + 2mM Dox	11.95	0.2856	41.86
DPPC + 2mM Ral	12.12	0.2463	49.24
DPPC + P84	8.050	0.1928	41.78
DPPC + 2mM Ral + P84	11.03	0.2248	49.08
DPPC + 0.5mM Dox + 0.5mM Ral + P84	12.62	0.2752	45.88
DPPC + 0.5mM Ral + P84	11.51	0.2590	44.45
DPPC + 0.5mM Ral	10.98	0.2312	47.50

Table 2. Enthalpy, entropy and the transition temperatures of liposomal formulations measured by nano DSC indicating the drug lipid interaction.

For drug-free DPPC control liposomes, a transition of 8.43 Kcal mol^{-1} occurred at 42.96 °C (Table 2). This transition is consistent with the conversion of the rippled gel phase to the liquid crystalline phase.[19] The inclusion of DOX into analogous DPPC vesicles did not significantly alter the T_m, suggesting that DOX was not associated with the bilayers and was instead incorporated in the aqueous core or partly adsorbed onto the surface. Although the PPO moieties of P84 were hypothesized to be present in the bilayers, the inclusion of P84 did not affect the T_m of DPPC vesicles. However, peak broadening was detected, suggesting a decrease in the cooperativity of the phase

transition as reported with the addition of cholesterol.[20] This peak broadening effect was only demonstrated in presence of P84 and/or MNP's that are coated with hydrophobic oleic acid. This is attributed to interdigitation of the PPO or oleic acid chains in the bilayers with absence of any ring structure which is the case with RAL. Upon addition of 2 mM RAL to liposome formulations; a significant phase transition of 12.12 Kcal mol^{-1} at 49.24 °C was observed. The addition of 0.5 mM RAL showed a transition of 10.98 Kcal mol^{-1} at 47.5 °C. This RAL-induced shift in to a higher T_m was directly proportional to the concentration of RAL included in liposome formulations. The higher T_m suggests more thermodynamic and mechanical stability of the liposomes. Various studies have revealed that an increase in mechanical stability is associated with an increase in bilayer rigidity and, in turn, colloidal stability.[21] Thus, RAL-containing liposomes were more stable than analogous, DOX-containing liposomes. The inclusion of MNP's (L/N ratio of 10,000/1) decreased the T_m significantly to 39.02 °C. This MNP-induced change in the T_m was inversely proportional to the concentration of MNP's incorporated into the vesicular systems (T_m = 41.21°C for L/N ratio of 20000/1). This is due to the hydrophobic interaction of the oleic acid coating on the MNP's with the lipid chains in the vesicle bilayer, thereby forming a less rigid lipid bilayer. Although the apparent reduction in bilayer rigidity might theoretically have led to leaky liposomes, drug release studies did not show any leakage from the MNP-containing liposomes in the absence of radio frequency (RF) heating.

The effect of incorporating DOX, RAL and P84 in DPPC liposomes was also illustrated by ^{31}P-NMR, as shown in Figure 5.

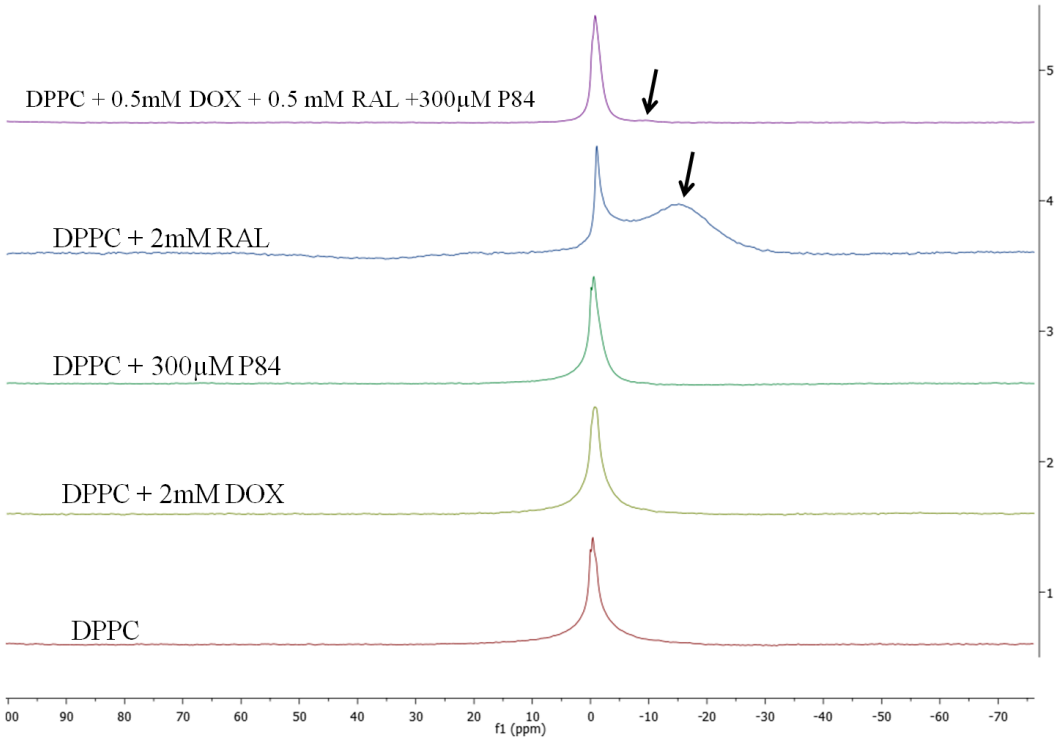

Figure 5. ^{31}P-NMR spectra after 60 K scans for liposomes containing 1) Blank DPPC 2) DPPC and 2 mM DOX and 3) DPPC and 300 µM P84 4) DPPC and 2mM RAL and 5) DPPC with 0.5mM RAL and DOX and 300 µM P84 dispersed in a 1:9 (D_2O:H_2O) solvent equilibrated at 37 °C. No shielding effect was detected for DOX or P84 containing liposomes. Black arrows indicate the shift in the upward field due to shielding effect of the aromatic rings present in RAL.

With a blank DPPC liposome, one single sharp peak was obtained, a characteristic indicator of small, unilamellar vesicles.[22] With the addition of either DOX or P84 to DPPC liposomes, neither a chemical shift nor a change in the shape of the NMR signal was detected. The presence of small, unilamellar vesicles was also confirmed with cryo-TEM imaging. Thus, it was concluded that, unlike RAL, neither DOX nor P84 affect the orientation or the environment of the phosphate head groups in the

liposomal bilayers. In contrast, with the incorporation of RAL, an additional resonance appears upfield of the DPPC resonance. This upfield resonance (black arrows) is the result of additional shielding due to the rigid aromatic rings of RAL which oriented themselves in the lipid bilayers in the proximity of the phosphate head group, which is associated with increased exposure of the phosphate groups to the vesicle surface. The magnitude of this shielding effect was directly proportional to the concentration of RAL incorporated into DPPC liposomes.[23] Thus, the orientation of different chemical species (such as drugs, polymer, and MNP's) in various regions of the liposomes was confirmed and in keeping with the desired optimized formulation design.

3.4. Drug release. DOX being hydrophilic due to the high polar surface area and protonated, charged tertiary amine, and RAL being relatively hydrophobic due to the presence of large domains of hydrophobicity, including a phenyl moiety, a benzothiophene heterocycle, and an aliphatic chain (Figure 6) were incorporated into different regions of the liposomes.

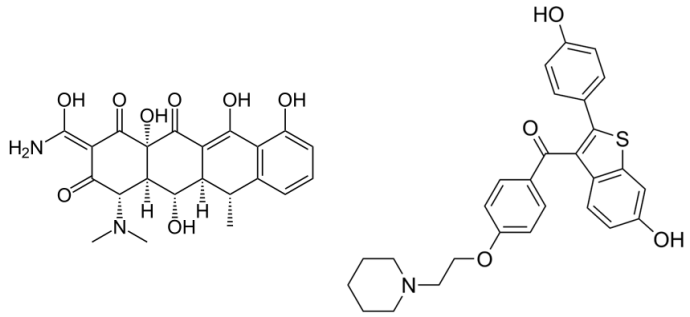

Figure 6. Chemical structures of DOX (left) and RAL (right).

DOX HCl has a high aqueous solubility and permeability and hence belongs to biopharmaceutical classification system (BCS) Class I, whereas RAL belongs to BCS Class II which comprises drugs of low solubility but high gastrointestinal permeability, and has a reported log P of 5.7.[24] The release of these drugs having different physiochemical properties from different regions of the liposomes was performed under physiological conditions with and without the use of an external magnetic field. Liposomal formulations were subjected to dialysis studies prior to the drug release in order to remove unentrapped drugs from the hydration media. The dialysis experiment was carried out until a constant drug concentration was obtained from assayed dialysate samples, indicating that equilibrium had been achieved and no unentrapped material was present in the dissolution sample. At the end of the dialysis experiment, mass balance equations were used to calculate the encapsulation efficiency of the liposomal formulations. At a 17 mM DPPC concentration, 1.88 mM

(94.56% theoretical) of DOX and 1.98 mM (99.35% theoretical) of RAL were successfully encapsulated.

While performing individual drug release studies, it was observed that DOX entrapped in the hydrophilic core was released from the liposomes, most likely due to passive diffusion driven by a concentration gradient across the vesicular lipid bilayer. About 1200 nM of DOX was released after 24 hours of dissolution. RAL, which was present within the lipid bilayers, showed even a lesser release in 24 hours (Figure 1). This underscores the apparent high affinity of RAL for DPPC bilayers as compared to DOX.

In order to form stable liposomes when using a combination of DOX and RAL in the same liposomal system, the concentration of each drug was reduced to 1 mM due to stability issues regarding liposomal aggregation. This system still failed to achieve the desired colloidal stability due to adsorbed DOX leading to aggregation. The concentration of the drugs used was further reduced to 0.5 mM which still showed aggregation. Hence, PL was incorporated into the liposomal bilayer in order to achieve stability by taking advantage of steric hindrance imparted by the PEO chains. This stabilized system was used for subsequent release studies, but no drug was detected in the dialysis or drug release media after 24 hours, suggesting complete drug encapsulation. It might be noted that these liposomal formulations displayed minimal leakage of the entrapped material, suggesting the advantage of minimal toxicity *in vivo* when using analogous formulations to entrap potent or toxic drugs with a narrow therapeutic index. In the interest of developing useful drug delivery systems, and in light of the complete absence of drug release from these two-drug containing

formulation, it was hypothesized that a trigger mechanism was needed so that the drugs would eventually be released from these liposomes. Accordingly, MNP's that could be subjected to an external electromagnetic field (due to their paramagnetic property), thereby inducing vibration and heating within the lipid bilayer, were successfully incorporated within the liposomal bilayers. Upon exposure to this external electromagnetic field, the MNP's would be expected to produce a local hyperthermia within the bilayers, thereby increasing the temperature above the T_m, and trigger drug release. MNP-containing liposomes did not show any drug release in the absence of an external magnetic field. However when subjected to a 30 min exposure to the external electromagnetic field and then stored at 37 °C, a release pattern was observed. As shown in Figure 7, the samples were collected at various time points such as 1, 3, 4, 20, 21 and 24 hours.

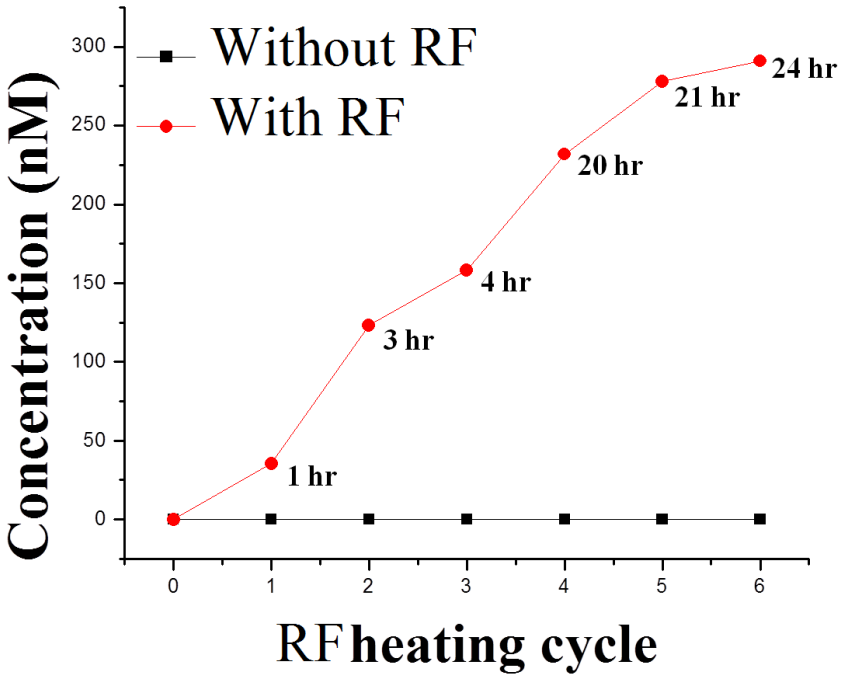

Figure 7. Rf- induced release of DOX from liposomes at 37 °C and at pH 7.4 in 137 mM PBS. Both DOX and RAL were encapsulated at 0.5 mM concentration.. The lipid: MNP ratio was 10000:1 that produced local hyperthermia and triggered the release of DOX. The red curve represents the drug release profile as a function of the RF heating cycle and the time points at which samples were collected in real time.

Before the collection of each sample, the formulations were subjected to 30 min. of RF exposure and stored at 37 °C for another 30 min. DOX release was independent of time and observed only after the exposure to the RF radiation. The rate and extent of DOX release from the liposomes was triggered by its exposure to an electromagnetic field. In contrast, electromagnetic irradiation had no effect on RAL release from lipid vesicles. RAL, being highly hydrophobic in nature and strongly interacting with the bilayer as demonstrated by NMR studies, did not show any release in vitro.

4. CONCLUSION

In the current investigation, we have successfully incorporated multiple drugs in the liposomal bilayers by taking advantage of their disparate physical-chemical properties and the different regions of DPPC liposomes. This combination therapy might be used for the treatment of various conditions that may require multiple drug administration for synergistic effect and in turn improved therapy. Poor stability is a general observation with liposomal systems which has been addressed by the use of PL's *via* steric hindrance that will maintain a homogenous particle size for an enhanced period of time ensuring a metered uniform dose at the time of administration. When using the combination of DOX and RAL, in order to enhance liposome stability, the drug concentrations had to be reduced from 2 mM to 0.5 mM. The presence of PL, MNP's and RAL in the bilayer had a pronounced effect on the suppression of DOX release. Under normal physiological conditions, the minimum cargo leakage is very desirable phenomena as it prevents various untoward systemic toxicities. Embedding MNP's in the bilayers gives the advantage of controlling and triggering the drug release with the aid of a physiologically invasion free magnetic field. *In vivo* studies using animal models might be conducted in order to better understand, refine, and optimize the performance of these delivery systems.

Supplemental Information

Calibration Curves

1) **Doxycycline HCl**

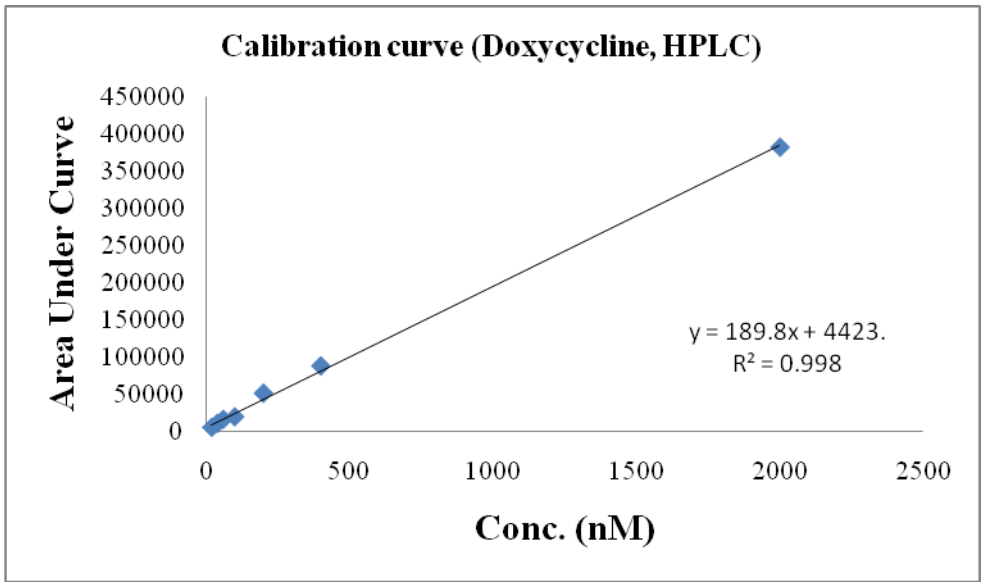

2) **HPLC chromatograms:**

a) 20nM

Area % Report

Data File: C:\EZChrom Elite\Enterprise\Projects\Test\Data\20nM dox3-24-2012 4-42-35 PMrkD-Rep1.met

Method: C:\EZChrom Elite\Enterprise\Projects\Test\Method\rkD.met

Acquired: 3/24/2012 4:45:00 PM

Printed: 3/26/2012 1:30:52 PM

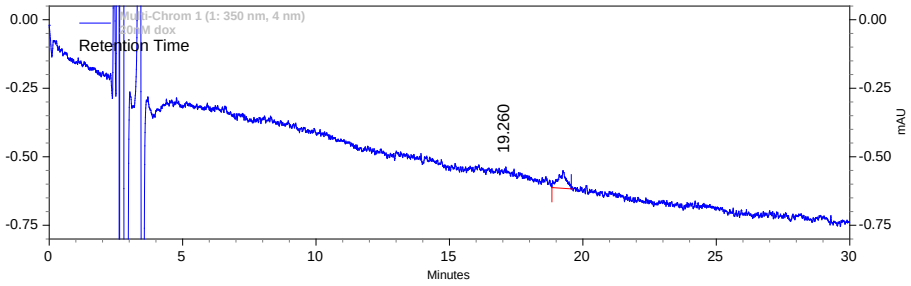

Chromatogram 1.

1: 350 nm, 4

nm Results

Retention Time	Area	Area %	Height	Height %
19.260	5260	100.00	257	100.00

Totals	5260	100.00	257	100.00

b) 200nM:

Area % Report

Data File: C:\EZChrom Elite\Enterprise\Projects\Test\Data\200nM dox3-22-2012 10-28-04 AMrkD.met

Method: C:\EZChrom Elite\Enterprise\Projects\Test\Method\rkD.met

Acquired: 3/22/2012 10:30:26 AM

Printed: 3/26/2012 2:25:21 PM

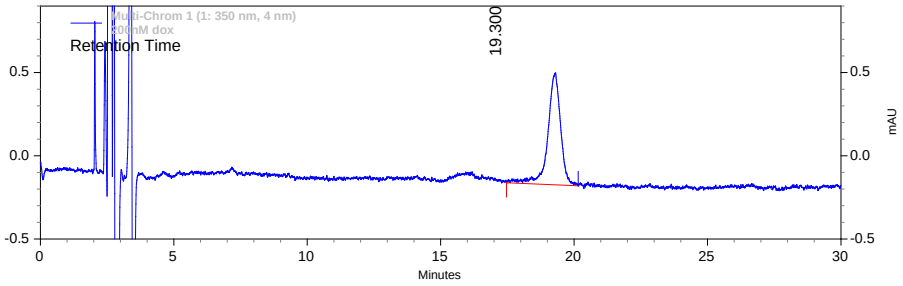

Chromatogram 2.

1: 350 nm, 4

nm Results

Retention Time	Area	Area %	Height	Height %
19.300	89903	100.00	2688	100.00

Totals				
	89903	100.00	2688	100.00

c) 2000nM

Area % Report

Data File: C:\EZChrom Elite\Enterprise\Projects\Test\Data\2000nM dox3-24-2012 11-12-52 PMrkD-Rep1.met

Method: C:\EZChrom Elite\Enterprise\Projects\Test\Method\rkD.met

Acquired: 3/24/2012 11:15:15 PM

Printed: 3/26/2012 3:16:24 PM

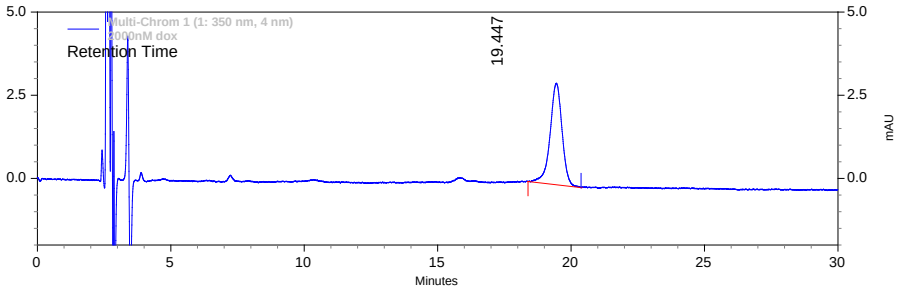

Chromatogram 3.

1: 350 nm, 4

nm Results

Retention Time	Area	Area %	Height	Height %
19.447	380930	100.00	12196	100.00

Totals	380930	100.00	12196	100.00

3) **Raloxifene HCl**

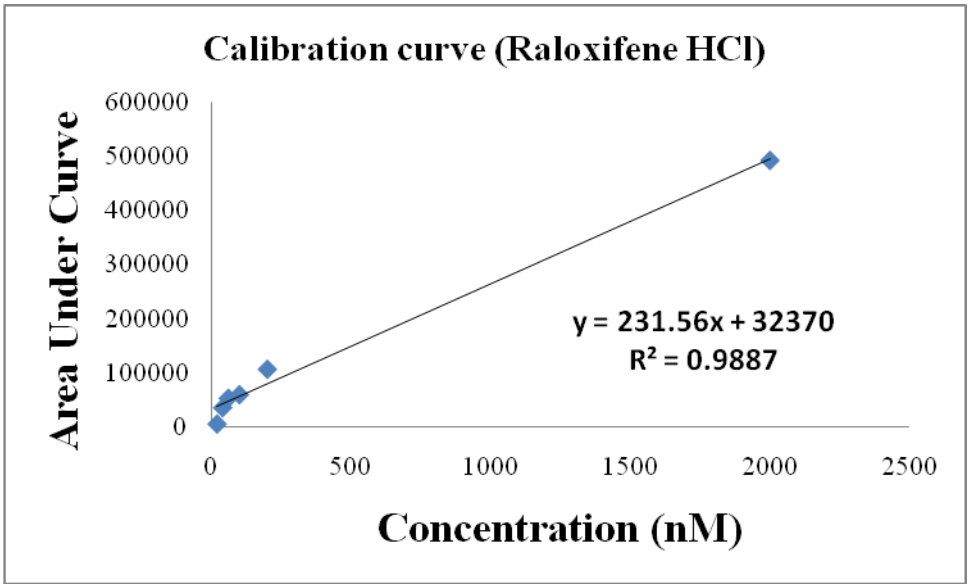

4) **HPLC chromatograms:**

a) 20nM

Area % Report

Data File: C:\EZChrom Elite\Enterprise\Projects\Default\Data\Swapnil\New calibration\20nM ralox in PBS5-31-2012 5-11-02 PM-Rep2.dat

Method: C:\EZChrom Elite\Enterprise\Projects\Default\Method\Swapnil\Rolaxifene_03_13_11.met

Acquired: 5/31/2012 5:13:21 PM

Printed: 6/1/2012 9:56:01 AM

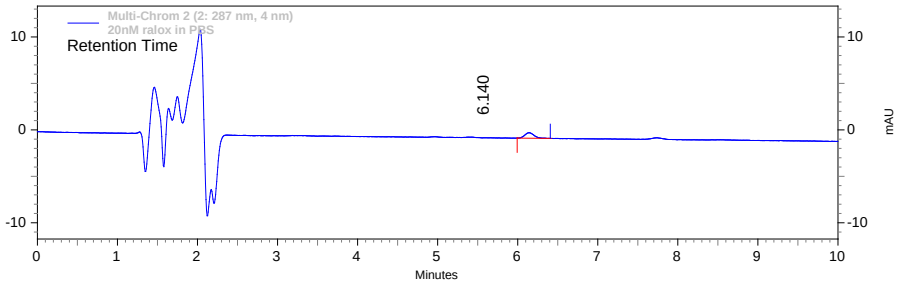

Chromatogram 1.

2: 287 nm, 4 nm

Results

Retention Time	Area	Area %	Height	Height %
6.140	18760	100.00	2347	100.00

Totals	18760	100.00	2347	100.00

b) 200nM

Area % Report

Data File: C:\EZChrom Elite\Enterprise\Projects\Default\Data\Swapnil\New calibration\200nM ralox in PBS5-31-2012 7-28-49 PM-Rep1.dat

Method: C:\EZChrom Elite\Enterprise\Projects\Default\Method\Swapnil\Rolaxifene_03_13_11.met

Acquired: 5/31/2012 7:31:10 PM

Printed: 6/1/2012 10:06:53 AM

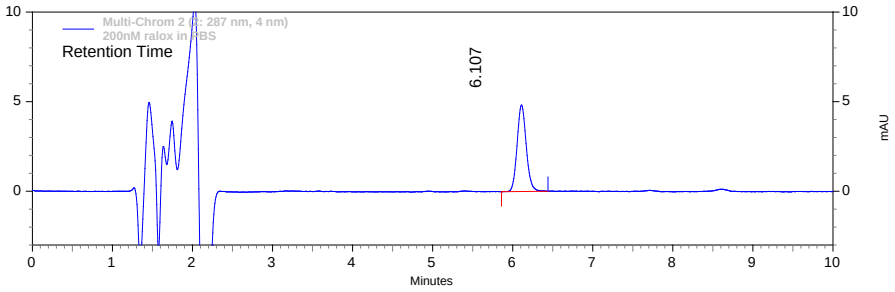

Chromatogram 2.

2: 287 nm, 4 nm

Results

Retention Time	Area	Area %	Height	Height %
6.107	153716	100.00	19297	100.00

Totals	153716	100.00	19297	100.00

c) 2000nM

Area % Report

Data File: C:\EZChrom Elite\Enterprise\Projects\Default\Data\Swapnil\New calibration\2000nM ralox in PBS5-31-2012 8-43-54 PM-Rep1.dat

Method: C:\EZChrom Elite\Enterprise\Projects\Default\Method\Swapnil\Rolaxifene_03_13_11.met

Acquired: 5/31/2012 8:46:15 PM

Printed: 6/1/2012 10:17:29 AM

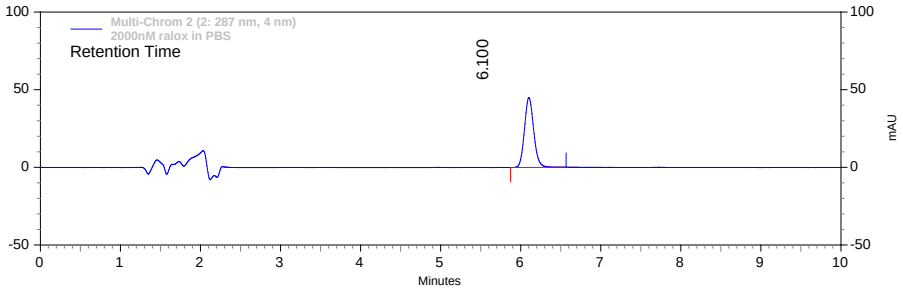

Chromatogram 3.

2: 287 nm, 4 nm

Results

Retention Time	Area	Area %	Height	Height %
6.100	1442786	100.00	180083	100.00

Totals	1442786	100.00	180083	100.00

5. REFERENCES

1. Lian, T.; Ho, R. J. *J Pharm Sci* **2001,** 90, (6), 667-80.

2. Randles, E. G.; Bergethon, P. R. *Langmuir* **2013,** 29, (5), 1490-7.

3. Yaroslavov, A. A.; Rakhnyanskaya, A. A.; Yaroslavova, E. G.; Efimova, A. A.; Menger, F. M. *Adv Colloid Interface Sci* **2008,** 142, (1-2), 43-52.

4. Sabin, J.; Prieto, G.; Ruso, J. M.; Hidalgo-Alvarez, R.; Sarmiento, F. *Eur Phys J E Soft Matter* **2006,** 20, (4), 401-8.

5. Liang, X.; Mao, G.; Ng, K. Y. *J Colloid Interface Sci* **2004,** 278, (1), 53-62.

6. Chapman, D.; Morrison, A. *J Biol Chem* **1966,** 241, (21), 5044-52.

7. Stark, B.; Pabst, G.; Prassl, R. *Eur J Pharm Sci* **2010,** 41, (3-4), 546-55.

8. Liang, X.; Mao, G.; Ng, K. Y. *J Colloid Interface Sci* **2005,** 285, (1), 360-72.

9. Wu, G.; Lee, K. Y. *J Phys Chem B* **2009,** 113, (47), 15522-31.

10. Zhao, Y.; Alakhova, D. Y.; Kim, J. O.; Bronich, T. K.; Kabanov, A. V. *J Control Release* **2013,** 168, (1), 61-9.

11. Nakano, M.; Kamo, T.; Sugita, A.; Handa, T. *J Phys Chem B* **2005,** 109, (10), 4754-60.

12. Yang, T.; Cui, F. D.; Choi, M. K.; Cho, J. W.; Chung, S. J.; Shim, C. K.; Kim, D. D. *Int J Pharm* **2007,** 338, (1-2), 317-26.

13. Ding, X.; Cai, K.; Luo, Z.; Li, J.; Hu, Y.; Shen, X. *Nanoscale* **2012,** 4, (20), 6289-92.

14. Oliveira, H.; Perez-Andres, E.; Thevenot, J.; Sandre, O.; Berra, E.; Lecommandoux, S. *J Control Release* **2013,** 169, (3), 165-70.

15. Schleich, N.; Sibret, P.; Danhier, P.; Ucakar, B.; Laurent, S.; Muller, R. N.; Jerome, C.; Gallez, B.; Preat, V.; Danhier, F. *Int J Pharm* **2013,** 447, (1-2), 94-101.

16. Chen, Y.; Bose, A.; Bothun, G. D. *ACS Nano* **2010,** 4, (6), 3215-21.

17. Bergstrand, N.; Edwards, K. *J Colloid Interface Sci* **2004,** 276, (2), 400-7.

18. Markus Johnsson, M. S., Go¨ran Karlsson, and Katarina Edwards. *Langmuir* **1990,** 15, (19), 6314-6325.

19. Quinn, P. J. *J Control Release* **2012,** 160, (2), 158-63.

20. Bolean, M.; Simao, A. M.; Favarin, B. Z.; Millan, J. L.; Ciancaglini, P. *Biophys Chem* **2010,** 152, (1-3), 74-9.

21. Anderson, M.; Omri, A. *Drug Deliv* **2004,** 11, (1), 33-9.

22. Cullis, P. R.; de Kruijff, B. *Biochim Biophys Acta* **1979,** 559, (4), 399-420.

23. **Amicangelo, W. R. L. a. J. C.** *Inorg. Chem.* **1998,** 37, (20), 5317-5323.

24. Tran, T. H.; Poudel, B. K.; Marasini, N.; Woo, J. S.; Choi, H. G.; Yong, C. S.; Kim, J. O. *Arch Pharm Res* **2013,** 36, (1), 86-93.

Chapter 2:

This manuscript is being prepared for submission to ***Lipid Research***.

The interactions and effects of di- and polyphenolic compounds on lipid vesicles.

Swapnil A. Malekar[1], Ashish L. Sarode[1], Alvin C. Bach II[1] and David R. Worthen[1, 2*]

[1]Department of Biomedical and Pharmaceutical Sciences, College of Pharmacy and

[2]Department of Chemical Engineering, College of Engineering, University of Rhode Island, Kingston, RI 02881

*Author to whom correspondence should be addressed:

495M Pharmacy Building,

7 Greenhouse Drive,

University of Rhode Island,

Kingston, RI 02881

Tel. 401-874-5016

email: dworthen@ds.uri.edu

ABSTRACT

Liposomes have been used in pharmaceutical industry for over 40 years and provide an attractive vehicle for delivery of hydrophilic as well as hydrophobic drugs. The hydrophilic drugs are entrapped in the aqueous core of the liposomes and do not tend to interact significantly with the bilayers in terms of packing parameters, dynamics, and state of aggregation. However, the opposite is true for hydrophobic additives and advances in analytical tools provide the opportunity to analyze these interactions. In this study, we investigate five hydrophobic small molecules (hydrophobic and phenolic) and their potential interactions with the DPPC bilayers. The liposomal processing parameters were kept constant with an aim to analyze the effects of different di- or polyphenolic compounds on DPPC liposomes. Various analytical tools, including differential scanning calorimetry and phosphorus- and proton nuclear magnetic resonance spectroscopy, were employed in order to evaluate the localization of the drugs along the thickness of the bilayer, and their effect on bilayer characteristics. It was observed that the molecules that tend to be located deep in the bilayers, do not assist in maintaining the hydrodynamic diameter of the vesicles as opposed to the drugs located in the vicinity of the glycerol region of the head group (within the bilayer). The molecules present in the upper region of acyl chains (C_1-C_{10}) prevented aggregation due to tight packing of the adjoining DPPC molecules.

1. INTRODUCTION

Liposomes have been used for a variety of applications, including therapeutics, diagnostics, and bioanalysis.[1] As described by Bangham et. al., liposomes are formed

by the phospholipid bilayers that encapsulate aqueous phases and are categorized as small unilamellar vesicles (20-100 nm), large unilamellar vesicles (50-400 nm) and multilamellar vesicles (400-5000 nm).[2] These phospholipids are known to be inert, non-immunogenic, and possess no intrinsic toxicity.[3] Due to the presence of both hydrophobic and hydrophilic domains, i.e., a bilayer and an aqueous core, liposomes have the capacity to encapsulate drugs, biologics, and various chemical substances of varying physiochemical properties within them.[4] The lipid bilayers constitute the second major region of liposomes, aiding in the incorporation hydrophobic substances which can be administered at effective concentrations without the use of any toxic organic solvents or solubilizing agents.[5]

The inclusion of hydrophobic materials has anecdotal effects on membrane dynamics and the phase behavior of liposomal bilayers that has been proved both experimentally and by molecular simulations.[6-10] In our previous study it was noticed that raloxifene hydrochloride (RAL), a selective estrogen receptor modulator (having estrogenic actions on bone and anti-estrogenic actions on uterus and breast[11]) increased the transition temperature of DPPC liposomes from 43 °C to 49 °C. This observation led to the investigation of the effect of compounds with similar physiochemical properties (such as hydrophobicity and di- and polyphenolic composition) as RAL, on DPPC bilayer dynamics, packing and, in turn, the colloidal stability of DPPC liposomes as a function of time. The purpose of this work was to determine the physiochemical changes in the bilayer properties with the addition of various hydrophobic drugs such as RAL, garcinol (GAR), quercetin (QTN), *trans*-resveratrol (RVR) and bisphenol A (BPA). GAR is a polyisoprenylated benzophenone known for its antibiotic and anti-

cancer activities.[12] QTN and RVR are plant-derived phenolics used for a variety of ailments such as inflammation, viral diseases, asthma, eczema, and cancer.[13-17] Although BPA is a toxic compound reported to cause behavioral alterations, preneoplastic lesions in prostate, and mammary gland and uterus[18], it was examined in this study not to serve a therapeutic but to appreciate its interaction with the DPPC bilayer owing to its hydrophobicity, aromatic, diphenolic character, and transoid conformation due to the presence of two geminal methyl groups.

The current investigation also includes localization of the drugs in various parts of the lipid bilayer which was determined by thermal, electrical and magnetic analysis (i.e. nano- Differential Scanning Calorimetry, zeta potential and ^{31}phosphorus- and proton nuclear magnetic resonance). Liposomes were prepared by a film rehydration technique and were then characterized under similar conditions for comparative analysis. It was observed that QTN and RVR were localized deep in the bilayer (C_{10}-C_{16} portion of acyl chains) that improved the packing properties of the chains but did not improve the colloidal stability. QTN and BPA were found to be associated with the glycerol region of the head group (C_1-C_{10}) and maintained the hydrodynamic radius over a period of 5 days. RAL formed larger vesicles as compared to other drugs but maintained the particle size and was found to be present in multiple stable orientations of the bilayer in the vicinity of the glycerol head groups.

2. MATERIALS AND METHODS

2.1. Materials.

1, 2-Dipalmitoyl-sn-glycero-3-phospocholine monohydrate (DPPC) was purchased from Corden Pharma (Colorado, USA). Quercetin (QTN) was purchased from Acros organics, raloxifene hydrochloride (RAL) from Fisher Scientific (Pittsburgh, PA), resveratrol (RVR) from CS Inc. (Danbury, CT), garcinol (GAR) from Enzo Life Sciences, NY and bisphenol A (BPA) from Sigma-Aldrich (St. Louis, MO). Phosphate buffered saline (PBS) tablets were purchased from MP Biomedicals (Solon, OH). All other reagents were purchased from Fisher Scientific and were of analytical grade.

2.2. Liposome preparation.

Vesicles were prepared at a 17 mM lipid concentration for all formulations. For the ^{31}P-NMR, the vesicles were made in 90:10 (water: D_2O), 100% D_2O for ^{1}H-NMR and 137 mM PBS for dynamic light scattering (DLS), Nano- Differential Scanning Calorimetry (nano-DSC) and zeta potential experiments. The vesicles were prepared as described by Chen *et al*.[19] The samples were further diluted to a lipid concentration of 1 mM for DLS and zeta potential, and 0.1 mM for nano-DSC using 137 mM PBS. Briefly, liposomes were prepared by dissolving 12.5 mg of DPPC in 1 ml of chloroform (for blank DPPC liposomes and GAR). Chloroform was removed by rotary evaporation at 50 °C (above the DPPC melting temperature) starting at 450 mbar for 30 min, then decreased to 300 mbar for 30 min, and finally 200 mbar for 30 min. This lipid film was kept under vacuum for 12 hours at room temperature to

remove traces of chloroform. It was then rehydrated with appropriate solvent for 2 hours at 50 °C. QTN, RVR, BPA along with DPPC were dissolved in methanol separately due to their limited solubility in chloroform whereas for RAL liposomes, RAL and DPPC were dissolved in a 1:1 ratio of chloroform: methanol due to the insolubility of RAL in pure chloroform. The organic solvents were removed by rotary evaporation at 50 °C (above the DPPC melting temperature) starting at 450 mbar for 30 min, then decreased to 300 mbar for 30 min, and finally 200 mbar for 30 min. This lipid film was kept under vacuum for 12 hours at room temperature to remove traces of organic solvents. The film was rehydrated with appropriate solvent at 50 °C for 2 hours. The resulting aqueous dispersions were then sonicated for 1hour using a bath sonicator maintained at 50 °C.

2.3. Nuclear Magnetic Resonance.

All NMR data were acquired on an Agilent NMRS 500 MHz NMR spectrometer using a 5mm NMRone probe. The probe temperature was thermostated at 37 °C for all experiments. Liposome formulations analyzed by NMR were prepared as previously described with the exception that 10% D_2O in water (^{31}P-NMR) or 100% D_2O (^{1}H-NMR) were used as a solvent in order to provide a deuterium lock signal. ^{31}P-NMR data were collected at 202.3 MHz for 60 K scans with a 35.7 kHz sweep width using 131 K data points. Acquisition time was 1.3 sec with a relaxation delay of 0.5 sec. A line broadening of 50 Hz was applied to all spectra. All spectra were indirectly referenced to H_3PO_4 set to 0 ppm. Data were acquired without spinning. ^{1}H-NMR data

were collected at 499.8 MHz using the conditions defined in figure captions. All NMR data were processed with mnova program V8.1 Mesterlab research SL.

2.4. Nano Differential Scanning Calorimetry (nano-DSC).

Nano-DSC was performed using a TA Instruments Nano DSC (New Castle, DE, USA). Samples at a concentration of 0.1 mM lipid were degassed under vacuum for 30 min before loading into a 0.6 mL capillary cell. The cell was then pressurized with nitrogen to 1 atm and equilibrated at 25 °C. The sample was scanned at 1 °C min^{-1} over a range of 10 °C to 60 °C.

2.5. Dynamic Light Scattering.

DLS measurements were performed using a Malvern Instruments Zetasizer Nano ZS with a backscattering detector angle of 173° and a 4 mW, 633 nm He-Ne laser (Worcestershire, UK). For size distribution studies, 1 ml of the liposome formulations was analyzed in an optical grade polystyrene cuvette at 37 °C. Before analysis, the samples were stored at 37 °C and then analyzed after 24 hours.

2.6. Zeta potential.

A small aliquot part of each formulation (17 mM DPPC) was diluted with 137mM PBS to give a final lipid concentration of 1 mM. Zeta potential values were then determined using a laser doppler procedure with a Malvern Instruments Zetasizer Nano ZS at 25 °C. Air drop interference was eliminated before measuring the zeta potential.

3. RESULTS AND DISCUSSION

In the previous chapter (in this dissertation), it was observed that RAL increased the T_m of DPPC liposomes significantly. It also had a pronounced effect on the ^{31}P-NMR peak with a shoulder in the upfield region indicating shielding of the NMR signal. This observation initiated the current work of exploring the interactions of various hydrophobic di- and poly-phenolic compounds (Figure 1) using thermal and magnetic analysis. The effect of the incorporation and localization of these drugs in the lipid bilayers on the colloidal stability of DPPC liposomes is also reported.

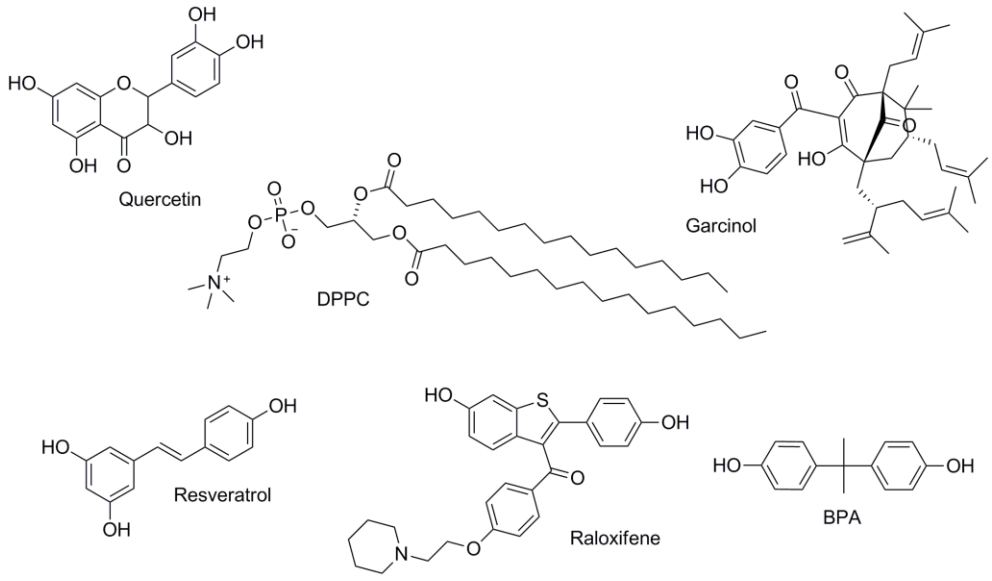

Figure 1. Chemical structures of different phenolic compounds and DPPC.

3.1. Thermal analysis.

Differential scanning calorimetry has been widely used in order to estimate the location of hydrophobic moieties in the liposomal bilayer as well as their interaction with the lipid.[20-22] The hydrophobic interior of a lipid bilayer is anisotropic in nature

due to a long range order of the acyl chains, which generates from cooperative interactions between these polymethylene chains. A cooperative unit exists in the gel phase of a bilayer due to transmission of motion among the fatty acid chains that are packed in a highly ordered hexagonal array.[23] The transition from gel to liquid crystalline phase suggests a change from nearly all trans to partially gauche conformation of C-C bonds in the chains.[24] This transition is an endothermic event and exhibits a specific profile in the DSC curve that provides information about the cooperative unit undergoing phase transition. Since the probability of C-C gauche conformation is higher in the end region of the chain (C_{10} and up), the center of a lipid bilayer tends to be more fluid due to disorder, and the interactions in the C_1-C_{10} region of the chain mainly regulate the size of the cooperative unit undergoing phase transition. The location of a hydrophobic molecule in different regions of the bilayer - phosphorylcholine, glycerol backbone, C_1-C_{10} methylene, and C_{10} and up methylene- and its interaction with these regions affect the cooperative unit and consequently the peak characteristics in the DSC profile. Thus, if a hydrophobic moiety is located in the C_1-C_{10} methylene region, it interacts with the cooperative unit and broadens the phase transition peak, whereas if it is located in the center (C_{10} and up methylene region) of the bilayer, the size of the cooperative unit is not affected and a sharper peak is detected. The packing of the cooperative unit can be altered in both cases, leading to an increase or decrease in the phase transition, which is also referred to as the melting temperature (T_m) of the bilayer. If a hydrophobic moiety interacts with the glycerol region of the bilayer, a shoulder peak is detected at a lower temperature along with the parent transition peak due to the formation of a new phase of its own smaller

cooperative units that don't coexist with the parent cooperative unit of the bilayer. On the other hand, a completely new peak appears due to formation of a new phase when chemical moieties such as cations and anions interact with the phosphorylcholine region of the bilayer.[25]

As shown in Figure 2, the liposomal bilayer of blank DPPC depicted its typical sharp peak at about 43 °C due to transition from a gel to liquid crystalline phase.

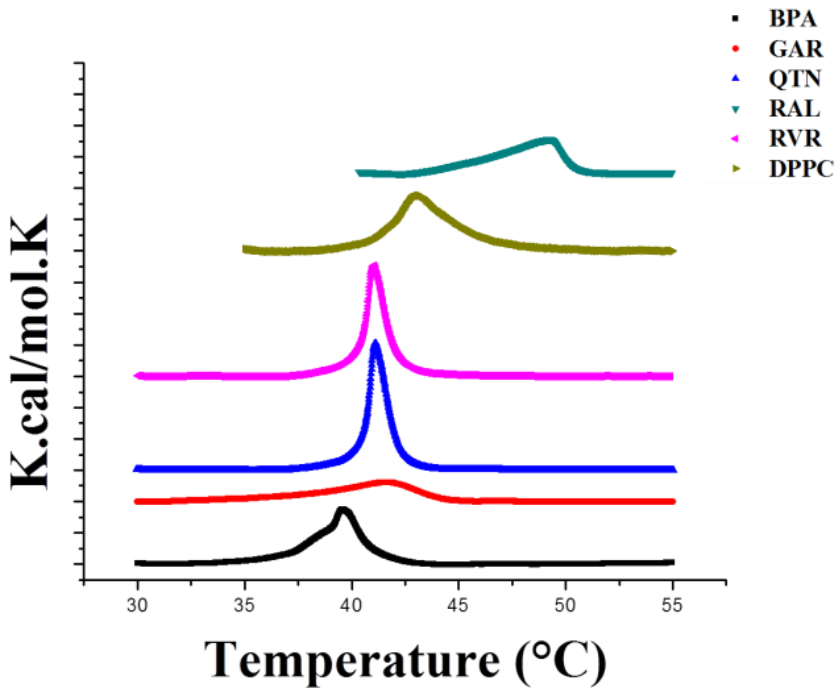

Figure 2. DSC endotherms depicting the effect of various drugs on the T_m of DPPC liposomes.

It can be estimated that RAL was located in the C_1-C_{10} methylene region of the bilayer and interacted with the parent cooperative unit, since the phase transition peak was slightly broadened after incorporation of RAL into the bilayer. Although the entropy

of this phase transition (Table 1) was only slightly increased, the enthalpy was substantially increased due to a significant increase in the T_m to about 49 °C.

Formulations	**ΔH (Kcal/mol)**	**ΔS [Kcal/(mol.K)]**	**T_m (°C)**
Blank DPPC	08.43	0.1963	42.96
DPPC + 2mM RAL	12.12	0.2463	49.24
DPPC + 2mM RVR	13.30	0.3242	41.05
DPPC + 2mM QTN	14.66	0.3565	41.12
DPPC + 2mM BPA	11.68	0.2952	39.58
DPPC + 2mM GAR	07.98	0.1917	41.62

Table 1. Enthalpy, entropy, and transition temperatures of different liposomal formulations containing di- and polyphenolic analytes.

Such a significant increase in the T_m due to the incorporation of RAL suggests that the packing of the cooperative unit was altered in such a way as to enhance the rigidity of the bilayer. Like RAL, GAR also exhibited a peak broadening effect, suggesting its incorporation into the C_1-C_{10} methylene region as well. In the case of GAR, however, the entropy, enthalpy, and the T_m were slightly decreased as compared to control, suggesting a slight reduction in the bilayer rigidity. A slight reduction in the T_m, broadening of the transition peak, and the appearance of a small shoulder at the lower temperature suggests that BPA was located in between the glycerol and the C_1-C_{10} methylene region and strongly interacted with the glycerol groups of DPPC molecules. Although the incorporation of RVR and QTN also depicted a slight reduction in the T_m, no peak broadening was detected, suggesting that the location of these drug

molecules was in the center (C_{10}-C_{16} methylene region) of the bilayer. Since the concentration of all of the polyphenolic compounds that were used in this work was relatively high (2 mM), it can be estimated that the center region of the bilayer could have been saturated with the drug in the case of both RVR and QTN. Consequently, it may have increased the cooperativity of phase transition leading to a sharpening of the transition peak and an increase in the entropy and enthalpy of phase transition.

3.2. ^{31}P-NMR.

The effect of incorporating RVR, RAL, QTN, BPA and GAR into DPPC liposomes was also illustrated by ^{31}P-NMR, as shown in Figure 3.

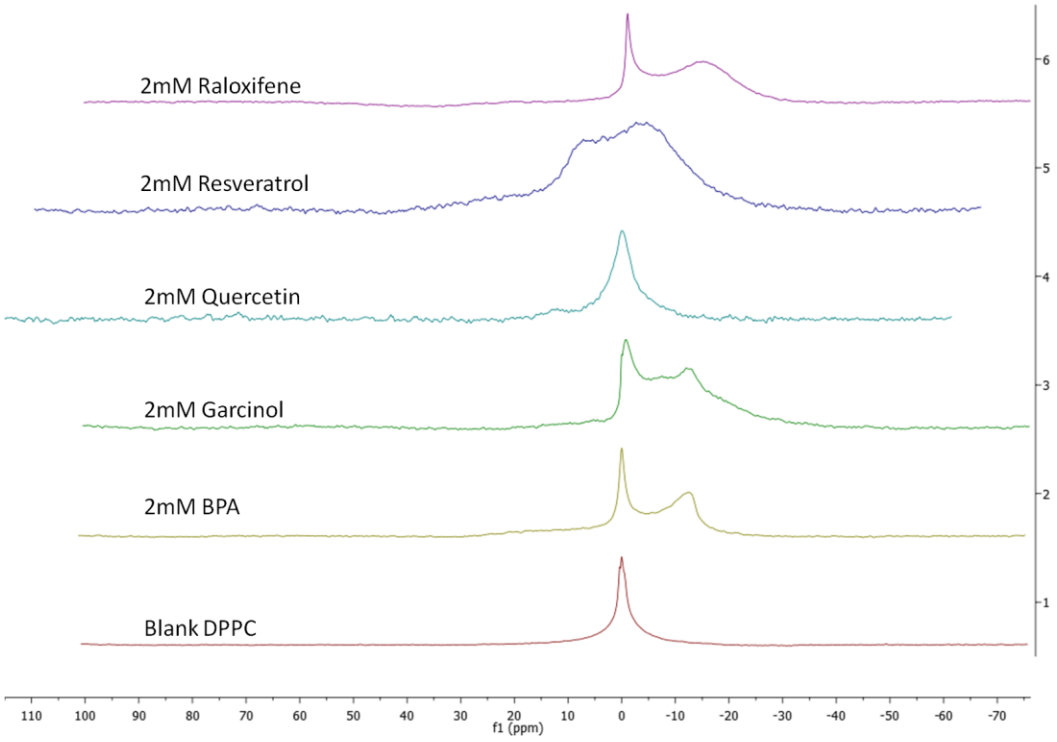

Figure 3. ^{31}P-NMR spectra after 60K scans at 37 °C in (9:1) water: D_2O as solvent, characterizing the interactions of the phenolic analytes with the phosphate head groups of DPPC liposomes.

With a blank DPPC liposome, one single sharp peak was obtained, a characteristic indicator of small, unilamellar vesicles.[26] The presence of small, unilamellar vesicles was also confirmed with cryo-TEM imaging (data not shown). With the addition of QTN to DPPC liposomes, no chemical shift was observed; however, the line shape broadened slightly. This peak broadening was unlikely to be caused by larger vesicles in solution because of the constant experimental procedure which produces morphologically similar liposomes (as indicated by DLS data). Thus, it is evident that there is a dynamic process involved with the phosphate head groups in the presence of QTN. However, the DSC data suggest that QTN is located deep in the bilayer, a situation that improves the orderliness of the acyl chains as it sharpens the transition peak. The NMR peak broadening is thus observed as an indirect effect on the change in the environment of the phosphate head groups due to an increase in the orderliness of the acyl chains and sharpening of the DSC curve. With the incorporation of RAL and BPA, an additional resonance appears upfield of DPPC resonance due to shielding and increased exposure of the phosphate groups. This upfield resonance is a result of additional shielding due to the rigid aromatic rings of RAL and BPA, which may orient themselves in the lipid bilayers in the proximity of the phosphate head groups. In addition, BPA has a shoulder at a lower temperature in the DSC curve and a peak broadening effect similar to RAL, suggesting localization of both the drugs in the vicinity of the glycerol moiety in the C_1-C_{10} chain region. GAR showed a similar effect with a much broader peak. This might be attributed to multiple stable interactions with the phosphate head groups. On the other hand, RVR showed the

broadest peak, which again indicates multiple stable interactions with the head group. However, RVR, like QTN, was presumed to be present deep in the bilayer at C_{10}-C_{16} region. Thus, there was no direct correlation between the DSC data and the NMR peak broadening, which might be due to the RVR-induced increase in the orderliness of the bilayers that in turn affect the phosphate head group environment. The orientation of different chemical species in various domains of liposomal bilayer was thus proposed.

3.3. ^{1}H-NMR.

All resonances in the blank DPPC liposome spectrum are broadened, consistent with the formation of vesicles. These results are consistent with general NMR principles and previous observations of vesicles.[27, 28] In this study, the phospholipid glycerol resonances were not observed. In the case of BPA, the glycerol methine resonance becomes clearly observable in liposomes loaded with BPA, as seen in Figure 4.

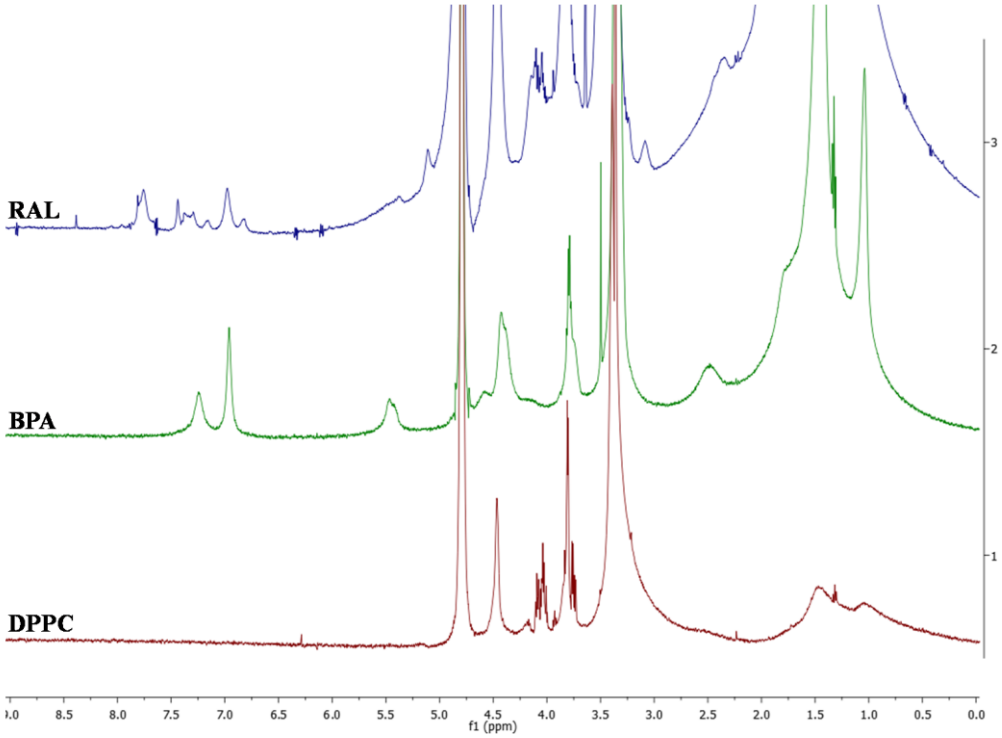

Figure 4. 1D ^{1}H-NMR spectra of RAL, BPA and blank DPPC liposomes showing aromatic peaks from the drug molecules.

The decreased line width is obtained because of an increase in local molecular motions in that region of the phospholipid. This would suggest that BPA is bound near the head group region. Also observed were the aromatic resonances of BPA in the NMR spectrum at 7.12 ppm (2, 6 and 2', 6') and at 6.84 ppm (3, 5 and 3', 5'). All of the aromatic resonances are broadened, which is indicative of the entrapment of BPA in the hydrophobic vesicle wall.[29] The BPA methyl resonance was not identified in the spectrum because of the overlapping DPPC resonances. In Figure 5(b), additional NOE are observed between the BPA resonance at 6.84 ppm and the -$N(CH)_3$ of the choline and a methylene near the carbonyl moiety of the acyl chains. This further supports the localization of BPA to near the glycerol region.

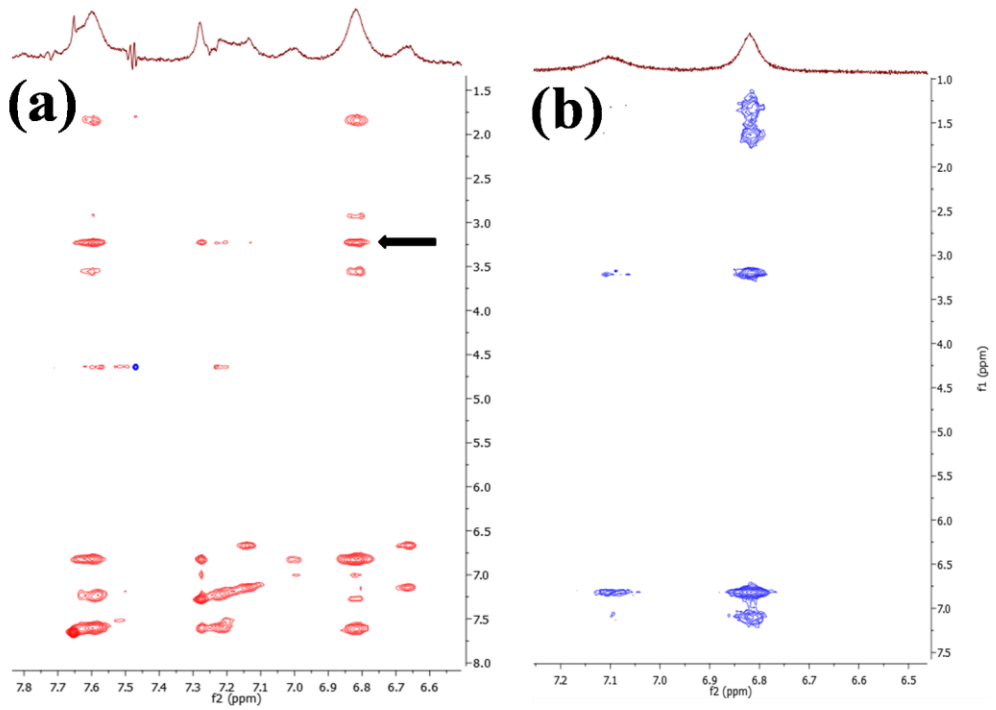

Figure 5. 2D ^{1}H-NMR spectra of (a) RAL and (b) BPA containing DPPC liposomes.

In the case of RAL (Figure 4), the vesicle resonances are similar to those observed for BPA-loaded vesicles. Aromatic drug resonances are observed with broadened line widths indicative of incorporation into the vesicles. The DPPC resonances are sharper in RAL-containing liposomes as compared to those observed in blank DPPC liposomes. The observed aromatic protons integrate to more than the expected value for one species of RAL. Assigning a value of one proton to the smallest aromatic resonance gives a total proton count of approximately 22, which is double the expected proton count for RAL. A possible explanation for this observation is that RAL is binding to the vesicle in two different ways which are not inter-converting on the NMR time scale. From Figure 5(a) we see more than the expected number of aromatic to aromatic NOE's in the 2D NOESY of RAL-containing liposomes. In bulk

solvent, RAL would be expected to exhibit three aromatic to aromatic NOE's. Two NOE's would arise from the protons of the two p-substituted phenyl rings and would be twice the intensity of the NOE between the ortho- protons of the benzothiophene ring of RAL. In RAL-containing liposomes we see NOE's for 5 aromatic to aromatic interactions and, while these interactions have not been assigned, it would seem unlikely they are all intramolecular NOE's, and some of the cross peak may represent exchange between multiple orientations of RAL in the vesicle wall environment. We also observe NOE's from two of the aromatic resonances to the *N*-methyl resonance of the choline head group (indicated by black arrow).

A single, broad aromatic resonance was observed in both the 1D and 2D data collected for RVR (data not shown). No resonances from GAR were observed in either 1D or 2D data collected. This indicates GAR and RVR are binding very tightly within the vesicle wall. Evidence of binding is seen because the -CH_2 and -CH_3 resonances from DPPC are sharper in GAR- and RVR-containing liposomes as compared to blank DPPC controls. This effect is similar to the other polyphenolics used in the study. In the case of QTN, five broadened aromatic peaks consistent with QTN structure are observed (Figure 6).

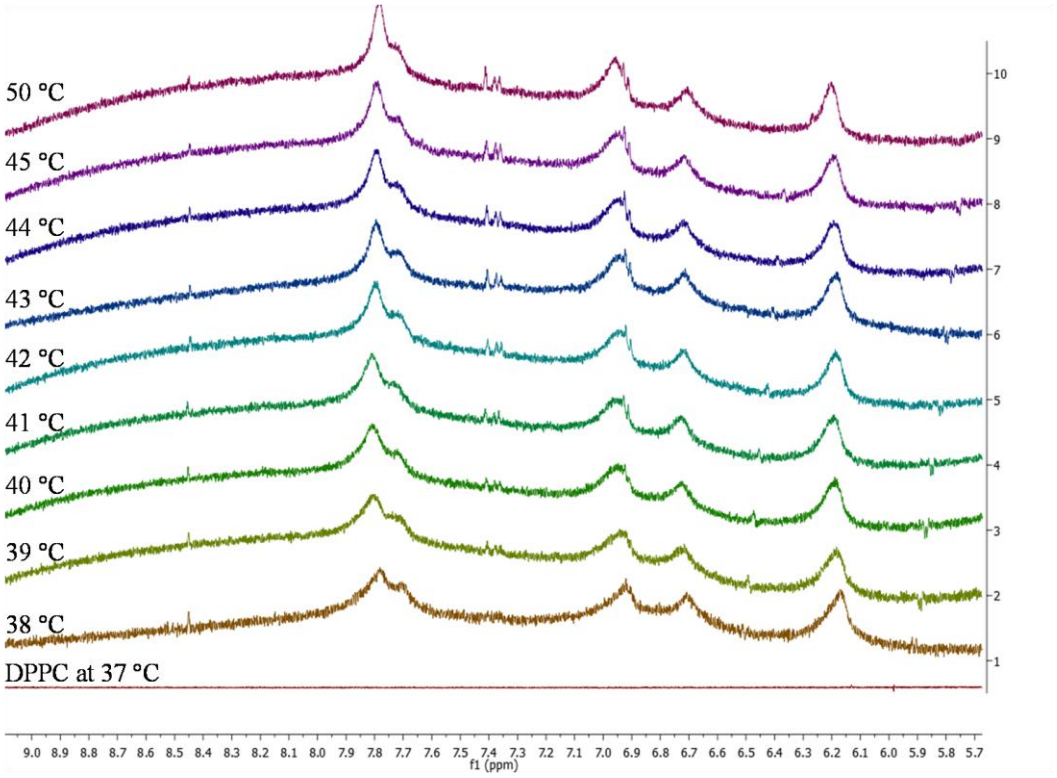

Figure 6. 1D ^{1}H-NMR spectra of (1) blank and (2-10) QTN-containing DPPC liposomes. No aromatic peaks were seen in blank DPPC liposomes whereas QTN peaks sharpened with the application of heat due to increased molecular mobility.

Again, the peak broadening indicates QTN binding to the vesicle wall. Also seen were changes in the DPPC spectrum indicative of drug binding. The -CH_2 and -CH_3 peaks are sharpened, as was observed with other phenolics assessed in this study. Also seen is a sharpened glycerol methine resonance as further proof of binding. The aromatic peaks observed were very broad. It was hypothesized that above the Tm of these vesicles, the molecular motion of QTN in the vesicle wall would increase, which could be indicated by sharper peaks. Thus, the formulations were heated from 38 °C to 45 °C (the Tm of QTN containing liposome was 41.12 °C) at 1 °C increments (10 min temperature equilibration time) and 1D NMR spectra were collected after each

temperature increment. Throughout the experiment, there was no significant chemical shift change for QTN resonances, indicating a consistent molecular environment. All five QTN resonances sharpened slightly in appearance as the temperature increased, a phenomenon indicative of increased molecular motion in the vesicle wall. As the temperature increased, sharp resonances consistent with QTN in bulk D_2O were also observed. The intensity of these resonances increased with increasing temperature, which suggests release of QTN from the vesicle wall into bulk solvent.

3.4. Particle size and zeta potential analysis:

The particle size analysis was conducted by DLS in triplicate over a period of time until aggregation was observed within the liposomes over a period of five days. As seen in Figure 7, several formulations maintained relatively consistent particle size save those containing QTN and RVR.

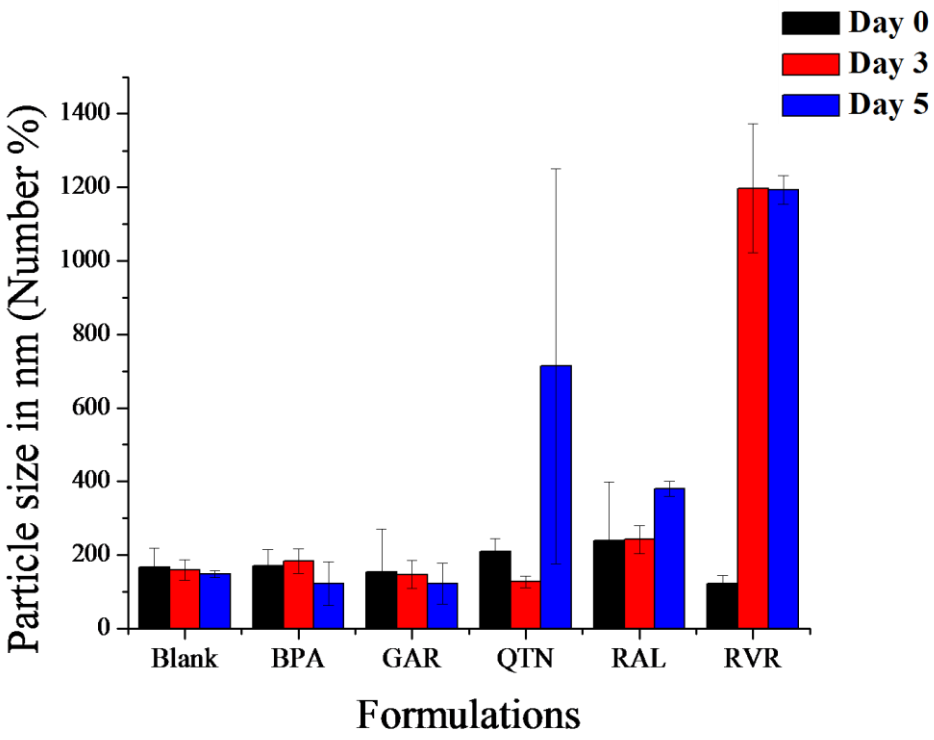

Figure 7. Liposome size (in nm) measured by DLS at 37 °C over a period of 5 days, indicating aggregation only with QTN- and RVR-containing DPPC liposomes.

It is evident that despite their effect on increasing the orderliness of the acyl chains of DPPC, QTN and RVR could not maintain the particle size and to the liposomes containing these compounds underwent aggregation. Thus, the localization of these and perhaps other hydrophobic compounds deep into the bilayer can have a significant effect on the stability of liposomes. In contrast, RAL, GAR, and BPA (located in the vicinity of the head group or C_1-C_{10} chain segment of DPPC) do not tend to alter the colloidal stability of liposomes which was evident from particle size data.

Zeta potential measurement was used to quantify the extent of external phosphate group exposure of liposomes in the presence of the phenolic compounds by measuring the surface charge. The zeta potential of blank DPPC liposomes over a period of 5 days was -2 ± 1 meV, which is consistent with the literature due to the adsorption of

OH^- ions from the surrounding buffer and exposure of the phosphate head groups.[30] The zeta potential of GAR-containing liposomes was -11 ± 2 meV over a period of 5 days, which could be attributed to the localization of the large GAR molecules in the vicinity of head group and increasing the exposure of phosphate head groups to the external media. This explains the DSC peak broadening effect of GAR due to a decrease in the cooperativity of mixing and its localization at the C_1-C_{10} region of the DPPC acyl chains. QTN and RVR were present deep into the bilayers while RAL and BPA might have aligned linearly with the acyl chains. Thus QTN, RVR, RAL and BPA did not have a significant change in the zeta potential of the liposomes. The zeta potential for these formulations was -1 ± 2 meV for a period of 5 days and was consistent for the mentioned period of time.

4. CONCLUSIONS

The localization of hydrophobic phenolics in DPPC liposomes was successfully characterized using a variety of analytical techniques. It has been demonstrated that the addition of various hydrophobic phenolics to liposomes may profoundly affect the characteristics of the vesicles and the bilayer organization. Despite certain similar physiochemical properties, these phenolics vary in geometry, flexibility, and molecular weight, and thus may be located in different regions (or even stable multiple positions as seen in the case of RAL) throughout the phospholipid bilayer. The phenolic compounds that were shown to be located deep in the bilayer do not appear to affect the colloidal stability of the liposomes.

SUPPLEMENTARY INFORMATION

1) Phenolics in bulk solvents (^{1}H-NMR)

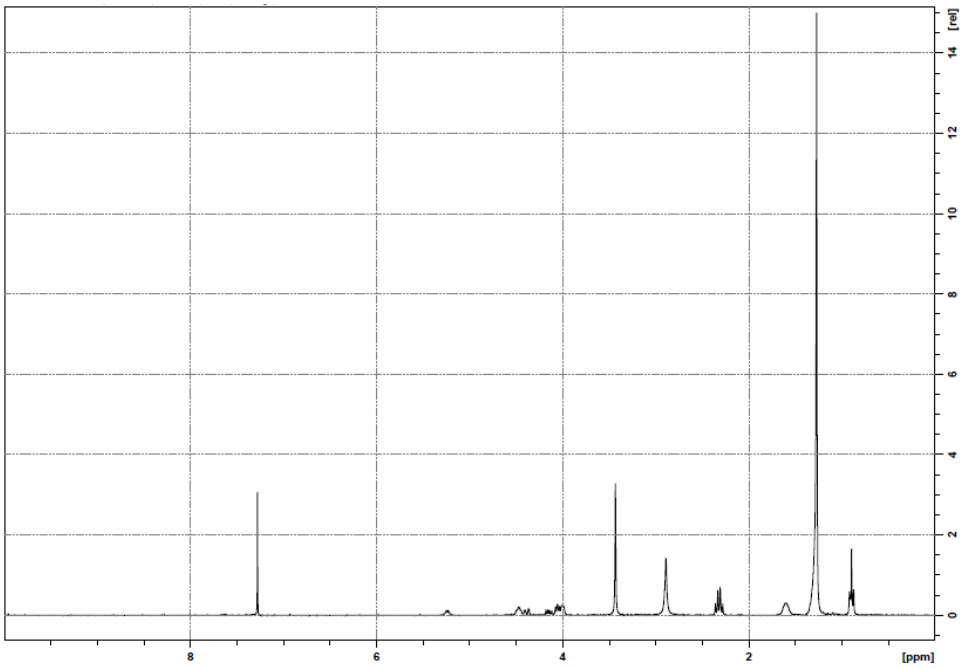

Spectra 1. DPPC in $CDCl_3$

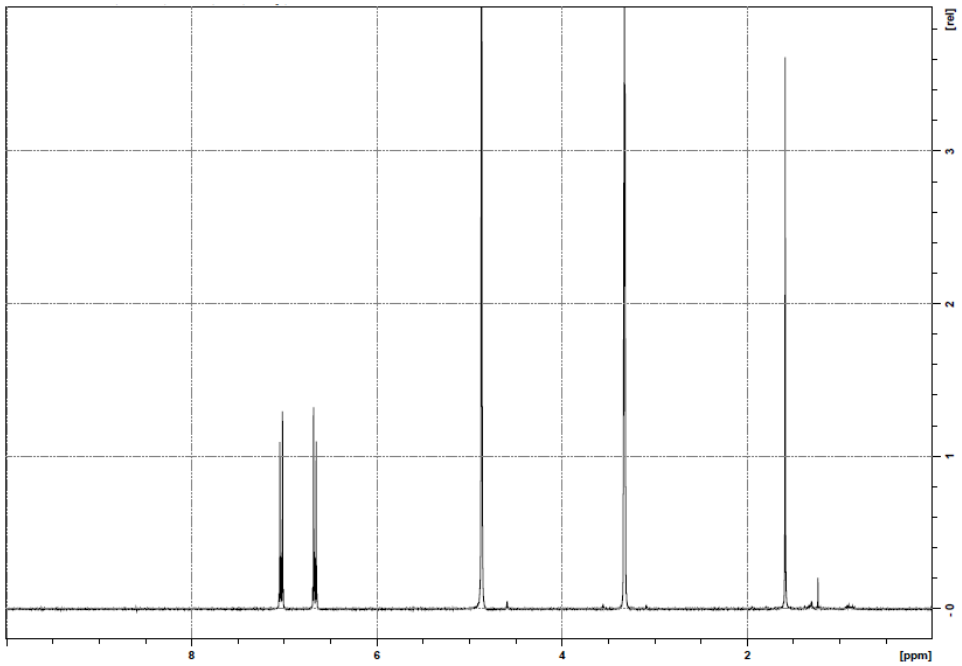

Spectra 2. BPA in MeOD

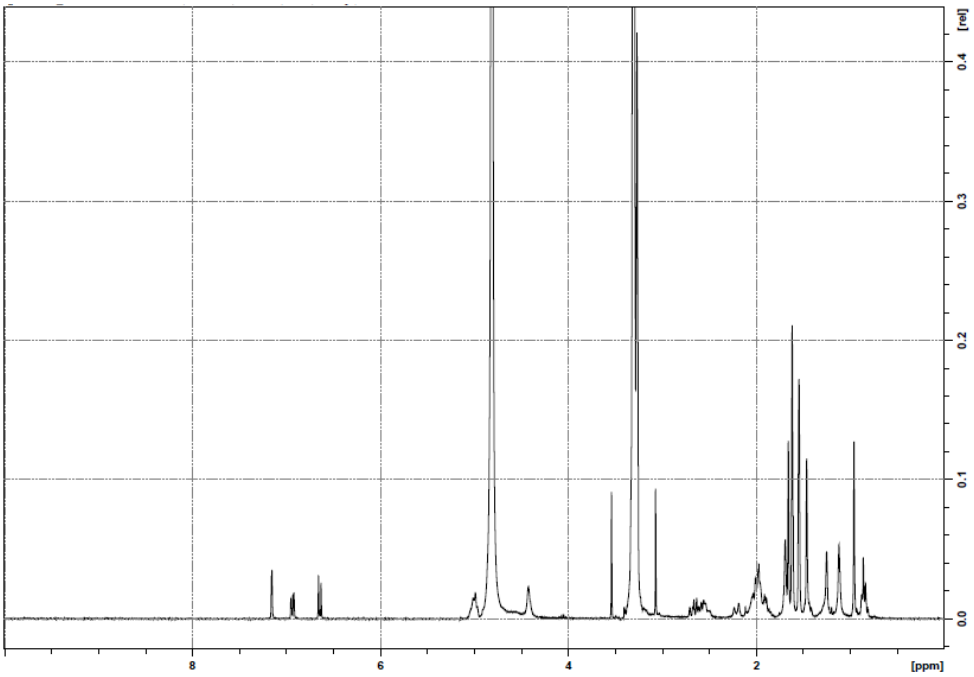

Spectra 3. GAR in $CDCl_3$

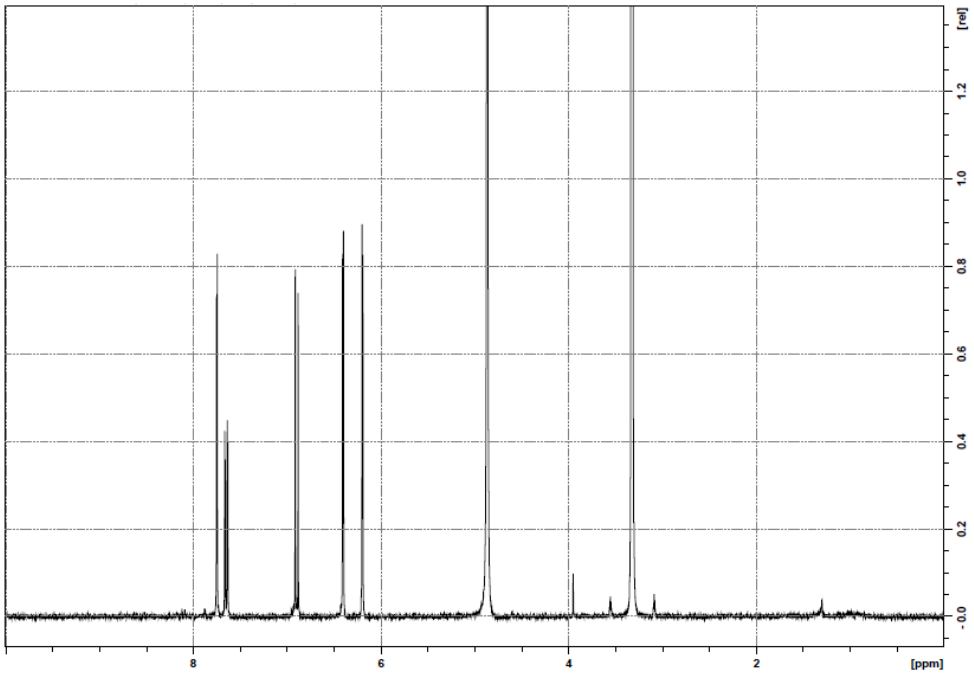

Spectra 4. QTN in MeOD

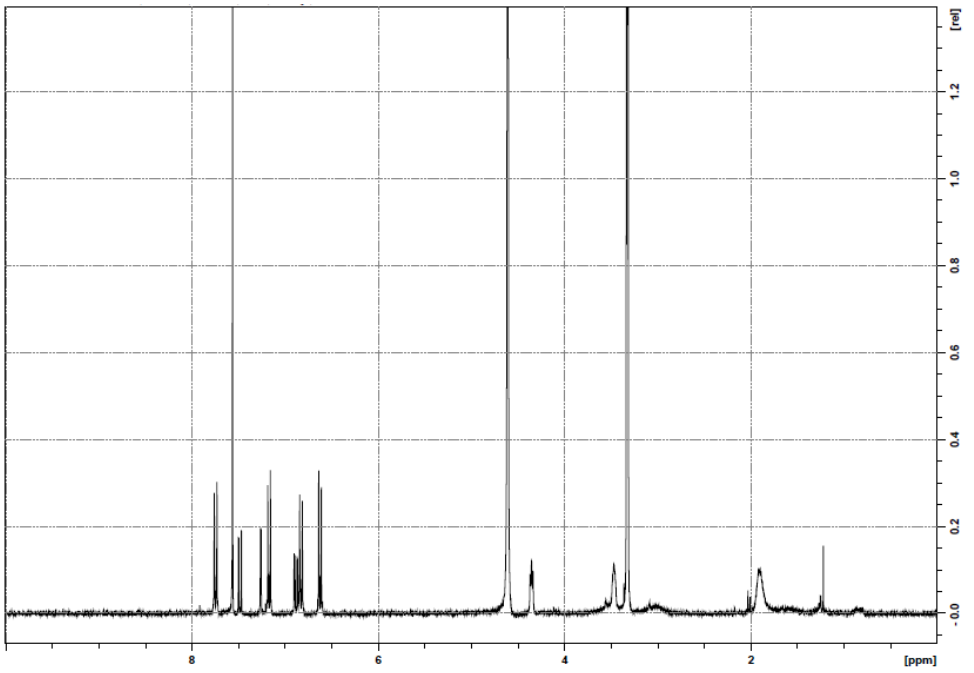

Spectra 5. RAL in $CDCl_3$:MeOD (1:1)

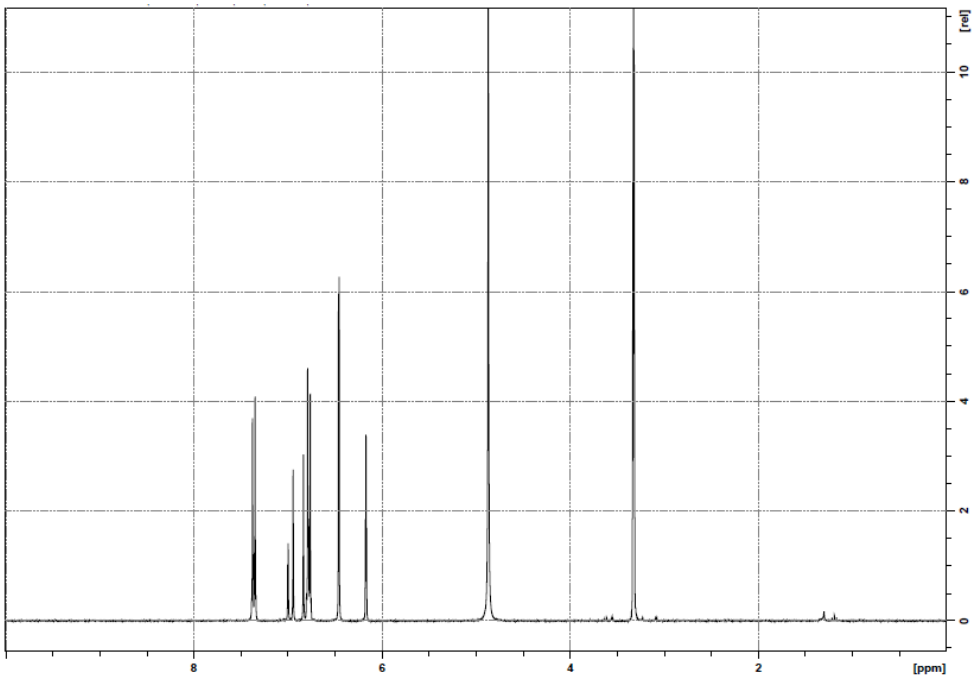

Spectra 6. RVR in MeOD

2) Phenolics in vesicles

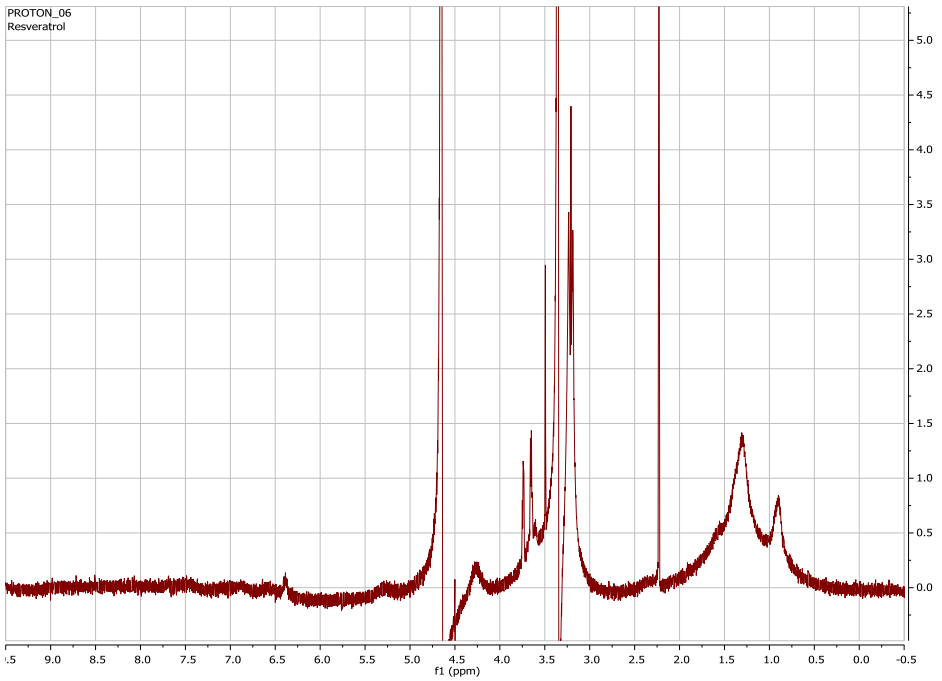

Spectra 1. RVR in DPPC

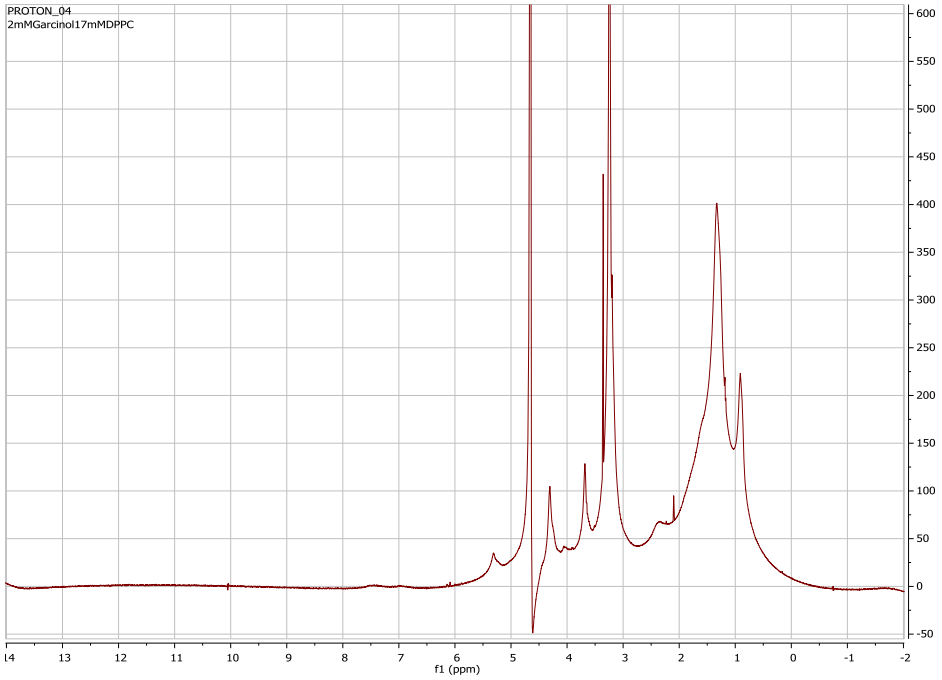

Spectra 2. GAR in DPPC

5. REFERENCES:

1. Edwards, K. A.; Baeumner, A. J. *Talanta* **2006,** 68, (5), 1421-31.

2. Bangham, A. D.; Standish, M. M.; Watkins, J. C. *J Mol Biol* **1965,** 13, (1), 238-52.

3. Immordino, M. L.; Dosio, F.; Cattel, L. *Int J Nanomedicine* **2006,** 1, (3), 297-315.

4. Gulati M, G. M., Singh S. *International Journal of Pharmaceutics* **1998,** 165, 129-68.

5. Coimbra, M.; Isacchi, B.; van Bloois, L.; Torano, J. S.; Ket, A.; Wu, X.; Broere, F.; Metselaar, J. M.; Rijcken, C. J.; Storm, G.; Bilia, R.; Schiffelers, R. M. *Int J Pharm* **2011,** 416, (2), 433-42.

6. Lee, H.; Kim, H. R.; Park, J. C. *Phys Chem Chem Phys* **2014,** 16, (8), 3763-70.

7. Cai, D.; Gao, W.; He, B.; Dai, W.; Zhang, H.; Wang, X.; Wang, J.; Zhang, X.; Zhang, Q. *Biomaterials* **2014,** 35, (7), 2283-94.

8. Pawlikowska-Pawlega, B.; Misiak, L. E.; Zarzyka, B.; Paduch, R.; Gawron, A.; Gruszecki, W. I. *Biochim Biophys Acta* **2013,** 1828, (2), 518-27.

9. Wu, R. G.; Dai, J. D.; Wu, F. G.; Zhang, X. H.; Li, W. H.; Wang, Y. R. *Int J Pharm* **2012,** 438, (1-2), 91-7.

10. Notman, R.; Noro, M. G.; Anwar, J. *J Phys Chem B* **2007,** 111, (44), 12748-55.

11. Vogel, V. G.; Costantino, J. P.; Wickerham, D. L.; Cronin, W. M.; Cecchini, R. S.; Atkins, J. N.; Bevers, T. B.; Fehrenbacher, L.; Pajon, E. R., Jr.; Wade, J. L., 3rd; Robidoux, A.; Margolese, R. G.; James, J.; Lippman, S. M.; Runowicz, C. D.; Ganz,

P. A.; Reis, S. E.; McCaskill-Stevens, W.; Ford, L. G.; Jordan, V. C.; Wolmark, N. *JAMA* **2006,** 295, (23), 2727-41.

12. Masullo, M.; Menegazzi, M.; Di Micco, S.; Beffy, P.; Bifulco, G.; Dal Bosco, M.; Novelli, M.; Pizza, C.; Masiello, P.; Piacente, S. *J Nat Prod* **2013**.

13. Cadena, P. G.; Pereira, M. A.; Cordeiro, R. B.; Cavalcanti, I. M.; Barros Neto, B.; Pimentel Mdo, C.; Lima Filho, J. L.; Silva, V. L.; Santos-Magalhaes, N. S. *Biochim Biophys Acta* **2013,** 1828, (2), 309-16.

14. Spedding, G.; Ratty, A.; Middleton, E., Jr. *Antiviral Res* **1989,** 12, (2), 99-110.

15. Park, H. J.; Lee, C. M.; Jung, I. D.; Lee, J. S.; Jeong, Y. I.; Chang, J. H.; Chun, S. H.; Kim, M. J.; Choi, I. W.; Ahn, S. C.; Shin, Y. K.; Yeom, S. R.; Park, Y. M. *Int Immunopharmacol* **2009,** 9, (3), 261-7.

16. Nothlings, U.; Murphy, S. P.; Wilkens, L. R.; Henderson, B. E.; Kolonel, L. N. *Am J Epidemiol* **2007,** 166, (8), 924-31.

17. Jung, M. K.; Hur, D. Y.; Song, S. B.; Park, Y.; Kim, T. S.; Bang, S. I.; Kim, S.; Song, H. K.; Park, H.; Cho, D. H. *J Invest Dermatol* **2010,** 130, (5), 1459-63.

18. Delclos, K. B.; Camacho, L.; Lewis, S. M.; Vanlandingham, M. M.; Latendresse, J. R.; Olson, G. R.; Davis, K. J.; Patton, R. E.; da Costa, G. G.; Woodling, K. A.; Bryant, M. S.; Chidambaram, M.; Trbojevich, R.; Juliar, B. E.; Felton, R. P.; Thorn, B. T. *Toxicol Sci* **2014**.

19. Chen, Y.; Bose, A.; Bothun, G. D. *ACS Nano* **2010,** 4, (6), 3215-21.

20. Joanne, P.; Galanth, C.; Goasdoue, N.; Nicolas, P.; Sagan, S.; Lavielle, S.; Chassaing, G.; El Amri, C.; Alves, I. D. *Biochim Biophys Acta* **2009,** 1788, (9), 1772-81.

21. Ikeda, A.; Kiguchi, K.; Shigematsu, T.; Nobusawa, K.; Kikuchi, J.; Akiyama, M. *Chem Commun (Camb)* **2011,** 47, (44), 12095-7.

22. El Maghraby, G. M.; Williams, A. C.; Barry, B. W. *Int J Pharm* **2005,** 292, (1-2), 179-85.

23. Alaouie, A. M.; Smirnov, A. I. *Biophys J* **2005,** 88, (2), L11-3.

24. Wang, G.; Lin, H. N.; Li, S.; Huang, C. H. *J Biol Chem* **1995,** 270, (39), 22738-46.

25. Jain, M.; Wu, N. M. *Journal of Membrane Biology* **1976,** 34, 157-201.

26. Cullis, P. R.; de Kruijff, B. *Biochim Biophys Acta* **1979,** 559, (4), 399-420.

27. Romberg, B.; Kettenes-van den Bosch, J. J.; de Vringer, T.; Storm, G.; Hennink, W. E. *Bioconjug Chem* **2006,** 17, (3), 860-4.

28. Pawlikowska-Pawlega, B.; Dziubinska, H.; Krol, E.; Trebacz, K.; Jarosz-Wilkolazka, A.; Paduch, R.; Gawron, A.; Gruszecki, W. I. *Biochim Biophys Acta* **2013,** 1838, (1), 254-65.

29. Pawar, B.; Joshi, M.; Srivastava, S.; Kanyalkar, M. *J Pharm Pharmacol* **2012,** 64, (6), 802-10.

30. Cevc, G. *Chemistry and Physics of Lipids* **1993,** 64, 163–186.

Chapter 3:

This manuscript is being prepared for submission to ***Journal of Controlled Release***.

The design and development of liposomes for the controlled delivery of multiple therapeutic drugs for pancreatic cancer.

Swapnil A. Malekar[1], Ashish L. Sarode[1], Qiushi Lin[1], Daniel Curzake[1], Xiaoquin Dong[1] and David R. Worthen[1,2*]

[1]Department of Biomedical and Pharmaceutical Sciences, College of Pharmacy and [2]Department of Chemical Engineering, College of Engineering, University of Rhode Island, Kingston, RI 02881

*Author to whom correspondence should be addressed:

495M Pharmacy Building,

7 Greenhouse Drive,

University of Rhode Island,

Kingston, RI 02881

Tel. 401-874-5016

email: dworthen@ds.uri.edu

ABSTRACT

In this study, gemcitabine was combined with the cyclooxygenase-2 inhibitor celecoxib in DPPC liposomes and assayed in vitro in order to assess the potential of these combination liposomes for the treatment of pancreatic cancer. Drug release from the liposomes was also controlled by an alternating high frequency AC magnetic field. Due to presence of hydrophobic iron oxide nano particles in the vesicular bilayer, local hyperthermia is produced that converts the rippled gel phase of liposomes to liquid crystalline phase. It was hypothesized that this phenomenon would induce the controlled release of these synergistic drugs from the liposomes. The liposomes were characterized in terms of drug localization by differential scanning calorimetry and ^{31}P-nuclear magnetic resonance spectrometry. Liposome morphology and size were confirmed by cryo-TEM and dynamic light scattering and remained in the sub-micron size range throughout the study. The MTT assay was performed in the human pancreatic cancer cell line BxPC-3 in order to assess cell viability. The results of the study indicated that liposomes containing both the drugs were more cytotoxic than single drug containing liposomes.

1. INTRODUCTION

According to the American Cancer Society, pancreatic cancer is the tenth most common cancer diagnosed in men and ninth most in women in the United States. An expected 45,420 new cases will be diagnosed in the United States of whom 39,590 will die in 2014[1], with a 5 year survival rate of 6%. Tumoral hypoxia (expression of hypoxia inducible factor -1) that correlates with an aggressive tumor phenotype and, in

turn, the development of chemoresistance, makes the treatment of certain pancreatic cancers particularly difficult.[2, 3] Gemcitabine (GEM), which is a first line of treatment for advanced pancreatic cancer, shows only moderate benefits due to chemoresistance that might be either intrinsic or acquired.[4, 5] However, the definitive underlying mechanism for GEM resistance in pancreatic cancer is unclear and maybe associated with atypical cell signaling pathways which are responsible for modulation in the cell cycle that leads to apoptosis of cancer or the inhibition of the conversion of GEM to its active form.[6-10] It has also been observed that there is an overexpression of cyclooxygenase 2 (COX-2) in more than 75% of invasive ductal carcinomas, which includes tumorigenesis of the pancreas.[11-17] Thus, the inhibition of COX-2 may be a complementary therapeutic target along with traditional anticancer therapies in pancreatic cancer.

Since the use of a single drug such as GEM through systemic administration has not produced satisfactory results in terms of tumor treatment, the use of multiple drugs should be given a high priority. The overexpression of COX-2 in pancreatic cancer and its interference with tumor angiogenesis provides an interesting rationale for using a combination of a COX-2 inhibitor such as celecoxib (CEL) with chemotherapeutic agent, such as GEM, in order to achieve much greater therapeutic efficacy.[18] A Phase II clinical trial of this combination has been proved to be effective, safe, and less toxic while treating the patients with advanced pancreatic cancers.[19]

For the above mentioned combination therapy, the dosage regimen includes oral CEL twice daily for 28 days and intra venous (IV) GEM for 65 minutes on days 1, 8 and 15.[20] This is mainly attributed to the difference in the physiochemical properties

of the drugs. CEL belongs to BCS class II with a low aqueous solubility of 5 µg/ mL and has a dissolution rate inhibited oral bioavailability of 22%.[21] On the other hand, GEM is a BCS Class I drug with an aqueous solubility of 83 mg/mL with a short plasma half-life of 45 minutes.[22] Also, an IV dose of GEM can produce various systemic side effects causing a hindrance in the treatment.[23] In order to overcome these various untoward effects, concurrent controlled delivery of these therapeutic agents is necessary. The synergistic combination of two drugs may reduce the toxicity of a single large dose of one drug whereas the second drug may maintain or improve desired therapeutic efficacy.

Liposomes are a promising tool for the concurrent delivery of multiple drugs owing to their ability to carry a drug payload in either the aqueous core (perhaps for hydrophilic GEM) or the lipid bilayer (for hydrophobic CEL).[24] In order to trigger the release of the liposomal contents, super paramagnetic iron oxide nano-particles (biocompatible and unreported *in vivo* toxicity) embedded in the liposomal bilayer are reported to cause local hyperthermia with the application of an alternating AC magnetic field.[25-27]

In this investigation, a synergistic combination of GEM and CEL was loaded into 1, 2-dipalmitoyl-sn-glycero-3-phospocholine monohydrate (DPPC) liposomes in order to evaluate the applicability of these nano devices to deliver multiple drugs. Oleic acid capped iron oxide nanoparticles (MNP's) were embedded within the liposomal bilayers for controlling the release of the cargo *via* the application of an electromagnetic field. These systems were tested *in vitro* in BxPC-3 (pancreatic cancer cell lines). It was observed that CEL potentiates the apoptotic effect of GEM (minimal

cell viability with the combination therapy) and the release of these drugs can be controlled from the liposomes using high frequency AC magnetic field.

2. MATERIALS AND METHODS

2.1. Materials. 1, 2-Dipalmitoyl-sn-glycero-3-phospocholine monohydrate (DPPC) was purchased from Corden Pharma (Colorado, USA). 1, 2-dioleoyl-*sn*-glycero-3-phosphocholine (DOPC) was purchased from Avanti Polar Lipids, Inc., (Alabama, USA).Gemcitabine hydrochloride (GEM) and Celecoxib (CEL) were purchased from Fisher Scientific (Pittsburgh, PA). Cellulose membranes (Spectra/Por MW cutoff 3500 Da), used for dialysis and drug release tests, were obtained from Spectrum Laboratories, Inc. (Houston, TX). Phosphate buffered saline (PBS) tablets were purchased from MP Biomedicals (Solon, OH). SPIO maghemite nanoparticles (5 nm, 24 mg ml^{-1} or 187.9 mM Fe_2O_3) dispersed in chloroform were purchased from Ocean Nanotech (Springdale, AR). On the basis of the density of maghemite (4.9 g cm^{-3}), 24 mg ml^{-1} is equivalent to 1.43×10^{17} particles ml^{-1}. All other reagents were purchased from Fisher Scientific and were of analytical grade.

2.2. Liposome preparation. Vesicles were prepared at a 17 mM lipid concentration for all formulations. For the ^{31}P-NMR, the vesicles were made in 90:10 (water: D_2O). The samples were further diluted to a lipid concentration of 5.6 mM for TEM, 1 mM for DLS and zeta potential, and 0.1 mM for nano-DSC. The procedure was same for all the formulations except for the step in which various components were added was differed for different formulations. GEM- containing liposomes were prepared by

dissolving 50 mg of DPPC in 4 ml of chloroform. Chloroform was removed by rotary evaporation at 50 °C (above the DPPC melting temperature) starting at 450 mbar for 30 min, then decreased to 300 mbar for 30 min, and finally 200 mbar for 30 min. This lipid film was kept under vacuum for 12 hours at room temperature to remove traces of chloroform. It was then rehydrated with GEM in 137 mM PBS for 1 hour at 50 °C. CEL-containing liposomes were analogously prepared. CEL and DPPC were dissolved in chloroform. The organic solvent was removed by rotary evaporation at 50 °C (above the DPPC melting temperature) starting at 450 mbar for 30 min, then decreased to 300 mbar for 30 min, and finally 200 mbar for 30 min. This drug-lipid film was kept under vacuum for 12 hours at room temperature to remove traces of organic solvent. The film was rehydrated with 137 mM PBS. The magnetic nano-particles (MNP's), CEL and GEM containing liposomes were prepared in a similar way by adding the MNP's [lipid/MNP (L/N) ratios of 5000:1 and 10000:1] to the organic solvent mixture containing lipid and CEL and following the film formation as described above using rotary evaporator and rehydrating the film with GEM in 137 mM PBS. The resulting aqueous dispersions were then sonicated for 1 hr using a bath sonicator at 50 °C.

2.3. Cryogenic Transmission Electron Microscopy (Cryo-TEM). Cryo-TEM samples were prepared at 25 °C using a Vitrobot (FEI Company), which is a PC-controlled robot for sample vitrification. Quantifoil grids were used with 2 μm carbon holes on 200 square mesh copper grids (Electron Microscopy Sciences, Hatfield, PA). Samples were first equilibrated within the Vitrobot at 25 °C and 100% humidity for 30

min. After immersing the grid into the sample, it was then removed, blotted to reduce film thickness, and vitrified in liquid ethane. The sample was then transferred to liquid nitrogen for storage. Imaging was performed in a cooled microscopy stage (Model 915, Gatan Inc., Pleasanton, CA) at 200 kV using a JEOL JEM-2100F TEM (Peabody, MA).

2.4. Energy dispersive X-ray scattering (EDS). EDS (Model INCAx-act, Oxford Instrument, K) was used to detect elemental iron from the magnetic nanoparticles within the iron oxide nanoparticle-loaded liposomes. EDS was conducted during cryogenic imaging with 158 s of live time and 92 s of dead time.

2.5. ^{31}Phosphorus- Nuclear Magnetic Resonance (^{31}P-NMR). The ^{31}P-NMR spectra were acquired on an Agilent NMRS 500 NMR spectrometer operating at 202.3 MHz using a 5mm NMRone probe. The probe temperature was thermostated at 37 °C for all experiments. Liposome formulations analyzed by NMR were prepared as previously described with the exception that 10% D_2O in water was used as a solvent in order to provide a deuterium lock signal. NMR data were collected for 60 K scans with a 35.7 kHz sweep width using 131 K data points. Acquisition time was 1.3 sec with a relaxation delay of 0.5 sec. The data were processed with mnova program V8.1 Mesterlab research SL. A line broadening of 50 Hz was applied to all spectra. Data were acquired without spinning.

2.6. Nano Differential Scanning Calorimetry (nano-DSC). Nano-DSC was performed using a TA Instruments Nano DSC (New Castle, DE, USA). Samples at a concentration of 0.1 mM lipid were degassed under vacuum for 30 min before loading into a 0.6 mL capillary cell. The cell was then pressurized with nitrogen to 1 atm and equilibrated at 25 °C. The sample was scanned at 1 °C min^{-1} over a range of 25 °C to 60 °C.

2.7. High Performance Liquid Chromatography (for quantification of dissolution). The HPLC system comprised a Hitachi La Chrome Elite equipped with a PDA detector and an automatic injector with a loop volume of 0.1 ml. For GEM quantification, a Phenomenex Nucleosil 10µ C18 100A (4.6 x 250 mm) column was used. The mobile phase consisted of 40 mM ammonium acetate/ acetonitrile (95/5) with a final pH of 5.5. The flow rate was 1 ml min^{-1} with an injection volume of 90 µl and a detection wavelength of 268 nm. The limit of detection of GEM using this method was 20 nM. The calibration curve in PBS was $R^2 = 0.999$. The column used for CEL quantification was an Atlantis dC18 3µm (150 x 4.6 mm) with a mobile phase comprising methanol/ water (72/28). The flow rate was 1 ml min^{-1} with an injection volume of 90 µl and a detection wavelength of 251 nm. The limit of detection was 20 nM and the calibration curve in PBS was $R^2 = 0.9997$. The R^2 linearity gives a correlation between the concentration of drug and the area under the curve of the HPLC chromatogram. R^2 value of 0.999 over a range of 20 nM to 200,000 nM suggests accurate quantification of drug derived from corresponding HPLC chromatograms.

2.8. Dynamic Light Scattering. DLS measurements were performed using a Malvern Instruments Zetasizer Nano ZS with a backscattering detector angle of 173° and a 4 mW, 633 nm He-Ne laser (Worcestershire, UK). For size distribution studies, 1 ml of the liposome formulations was analyzed in an optical grade polystyrene cuvette at 37 °C.

2.9. Dialysis. The dialysis experiments were conducted at room temperature (25 ± 0.5 °C) using 3.5 kDa tubular cellulose acetate membranes for 24 hours in 137 mM PBS with constant stirring and replacement of the dissolution media. The dissolution media was collected and analyzed by HPLC for unencapsulated drug in order to calculate the drug loading capacity of the liposomes. The experiments were carried out at 24 ± 0.5 °C and a pH of 7.4 with a stirring speed of 75 rpm using a 0.5 inch magnetic stirrer. Fresh media was replaced after the sampling was done at regular time intervals in order to maintain a sink condition.

2.10. Cell line study and MTT assay. BxPC-3 cells were incubated at 37 °C under a humidified atmosphere with 5% CO_2 and 95% air in RPMI 1640 medium (Gibco, USA), 10% Fetal Bovine Serum (FBS) (Gibco, USA) with 50 units per ml penicillin and 50 µg/mL streptomycin. The cells were seeded in a 24 well plate at optimum confluence (5 x 10^4 cells/ well). Two different plates were prepared at the same time under similar conditions and loaded with similar liposomal formulations. One plate was subjected to RF heating using pancake-style copper heating coil (3 turns) and heating was conducted using a 1kW HotShot (Amerithem Inc., Scottsville, NY)

operating up to 250 A and 170 kHz. The RF exposure was conducted at 4, 8, 20, 24, 28 and 40 hours for 30 minutes each. The other plate was left at room temperature outside the incubator (control) for the same amount of time as the plate subjected to RF heating. The cell viability was evaluated by MTT assay. Briefly, 100 µl MTT solution was added into each well of the 24-well plate. Gently the plate was stirred on a shaking platform at 150 rpm for 5 min, and returned to the incubator. After 3 h, MTT containing medium was removed and the fromazan was dissolved in 500 µl dimethyl sulfoxide (DMSO), and gently stirring the plate on the shaking platform for 5 minutes. The plate was then placed in the plate reader and absorbance was measured at 570nm and 690 nm. The background absorbance at 690 nm was subtracted from the reading at 570 nm to get the net absorbance value for each well.

3. RESULTS AND DISCUSSION

3.1. Morphological characterization:

Characterization of the vesicles in terms of morphology and elemental analysis was essential to evaluate the effect of two drugs *viz.* GEM and CEL and MNP's on their size, shape, and contents. In order to confirm the inclusion of MNP's in the bilayers of the vesicles (L/N ratio was 10,000: 1), an EDS scan was performed in areas that had liposomes and no prevalent MNP aggregates.

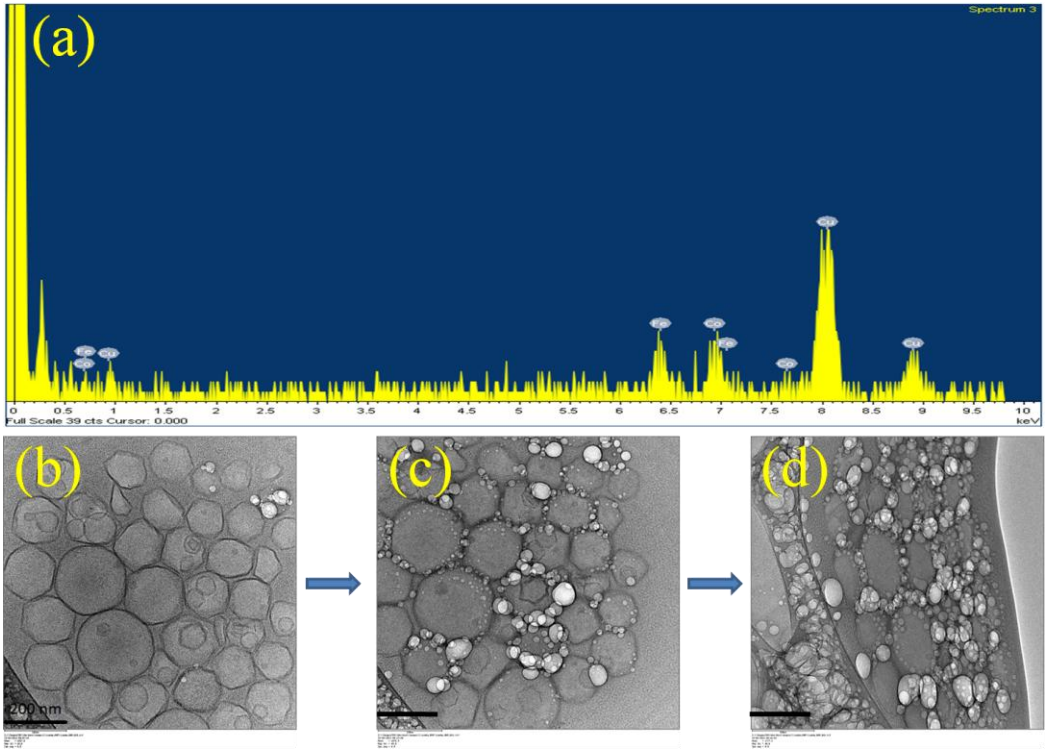

Figure 1. EDS scan (a) conforming presence of iron oxide in the liposomes. Cryo-TEM images (b, c and d) indicating morphology of liposomes and showing melting at the bilayer. The scale bar is 200 nm.

Figure 1(a) shows distinct iron peak at 6.4 keV (K_α) and 6.9 keV (K_β) confirming the presence of MNP's in the bilayers. No iron peaks were seen in the formulations not containing MNP's (data not shown). As seen in Figure 1(b), inclusion of the drugs and MNP's did not affect the morphology of the liposomes. Small unilamellar vesicles with a vesicle wall thickness of 5 nm were distinctly observed. After 1 minute exposure to the electron beam, the film starts melting at the bilayers as seen in Figure 1(c) which has a high concentration of MNP's. On continuous exposure for one more minute, the film starts melting with distinct bubbles at the bilayers as seen in Figure 1(d). Thus, it was confirmed that small unilamellar vesicles containing two drugs and MNP's were successfully formulated.

3.2. Drug-lipid interactions:

The drug-lipid interactions were thermally analyzed using Differential Scanning Calorimetry (nano-DSC) and magnetically by phosphorus- nuclear magnetic resonance (^{31}P-NMR) spectrometry. The concentrations of individual drugs in these experiments were kept higher than those in the cell line study for ease of quantification. As seen in Figure 2, blank DPPC liposomes show a sharp transition temperature (T_m) at 43 °C. This transition corresponds to the conversion of the rippled gel phase of the liposomal bilayers into the liquid crystalline phase.

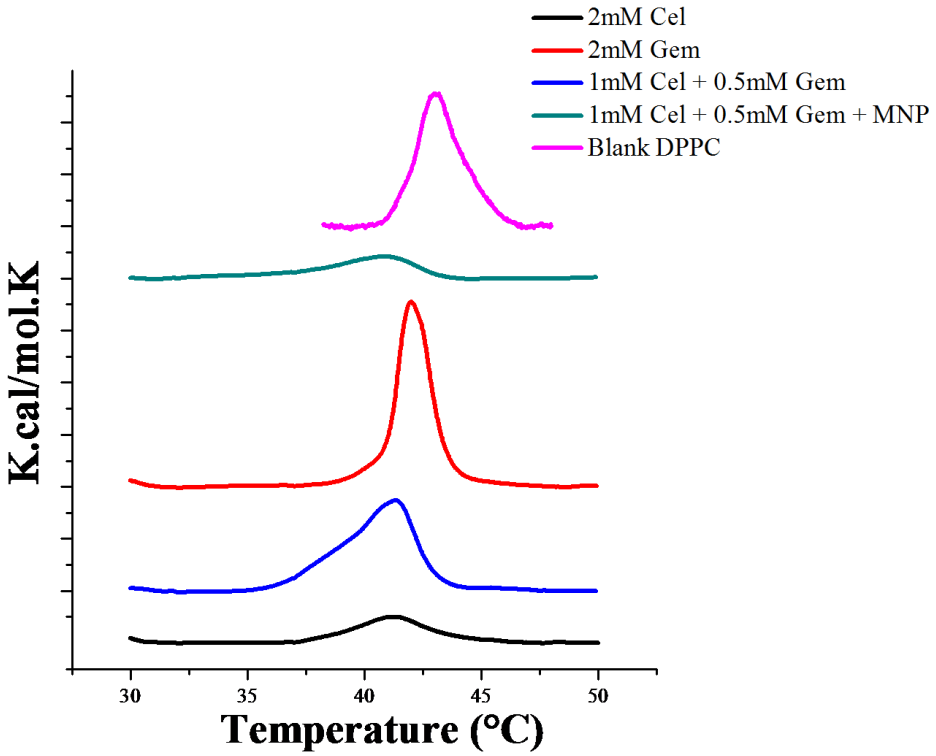

Figure 2. Nano-DSC thermographs indicating the presence of CEL and MNP's in the liposomal bilayer evident from peak broadening and shouldering corresponding to increased cooperativity of mixing and alteration in the bilayer packing.

Upon the addition of 2mM GEM, the peak sharpened slightly and the $T_{m\ moved}$ towards left on the temperature scale. This could be due to partitioning of some GEM into the bilayer despite its hydrophilicity. The peak sharpening effect is attributed to the localization of the drug (GEM in this case) in the much disordered C_{10} to C_{16} methylene region of the DPPC i.e. the centre of the bilayer.[28] Since it did not appear to interact with the much more ordered C_1-C_{10} chain of DPPC, it did not affect the shape of the curve significantly. However, this effect is evident with the addition of hydrophobic CEL and oleic acid coated MNP's. The peak broadening effect was a function of concentration of the hydrophobic content in the bilayer (2mM CEL formulation had a broader peak than 1mM CEL). This phenomenon could be attributed to the interaction of the drugs and hydrophobic MNP's with ordered C_1-C_{10} region of the lipid chain resulting in the decrease in the cooperativity of mixing.

The localization of the drugs in different domains of the liposomes was also demonstrated by ^{31}P-NMR (Figure 3).

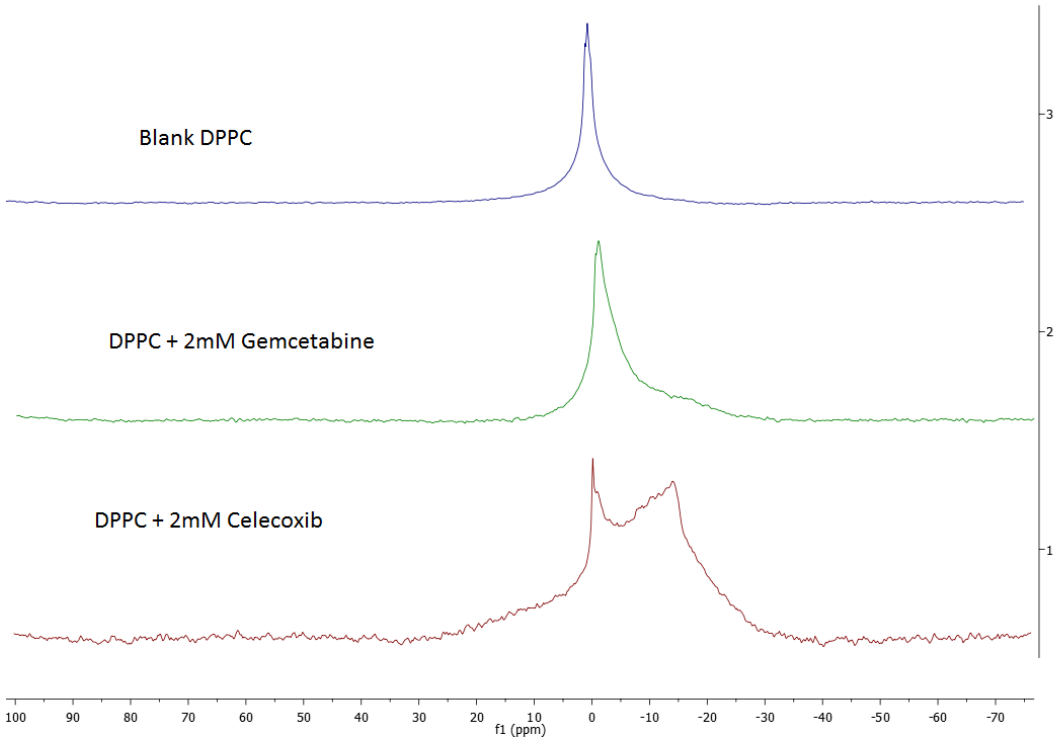

Figure 3. ^{31}P-NMR spectrum indicating presence of CEL in the vicinity of the phosphate head groups as evidenced by the additional resonance seen in the upfield region.

In the case of blank DPPC liposomes, a single, sharp peak characteristic of small unilamellar vesicles is seen (confirmed by TEM). [29] There was no evident change in the shape or location on the X-axis (indicator of chemical shifts) for GEM containing liposomes. This suggests that GEM did not interact with the phosphate head group region and hence did not alter the environment. However, with the addition of CEL, an additional resonance was observed in the upfield region of the spectra. This might be due to increased exposure of the phosphate head groups to the surrounding media. The additional resonance is an effect of the shielding due to the presence of aromatic rings of CEL in the vicinity of phosphate head groups[30].

3.3. Cell line study.

In order to evaluate the cytotoxicity of the combination of drugs, various formulations were prepared that were incubated with BxPC-3 cells for 48 hours with and without the magnetic RF heating. The results of the MTT assay suggest that there was no significant difference in the cell viability with or without the application of the magnetic field when the combination of drugs was loaded in the liposomes. As seen in Figure 4, at 17 mM DPPC concentration, using 3 different volumes of the formulations, the cytotoxicity increased with the increase in the loading volume of liposomes. These results suggest that at higher drug concentrations, RF heating did not provide a useful tool as the drug release was mainly governed by concentration gradient across the bilayer. Also, it was assumed that higher MNP concentration (L/N ratio of 5,000: 1) might have produced leaky liposomes that released the drugs without the application of RF heating.

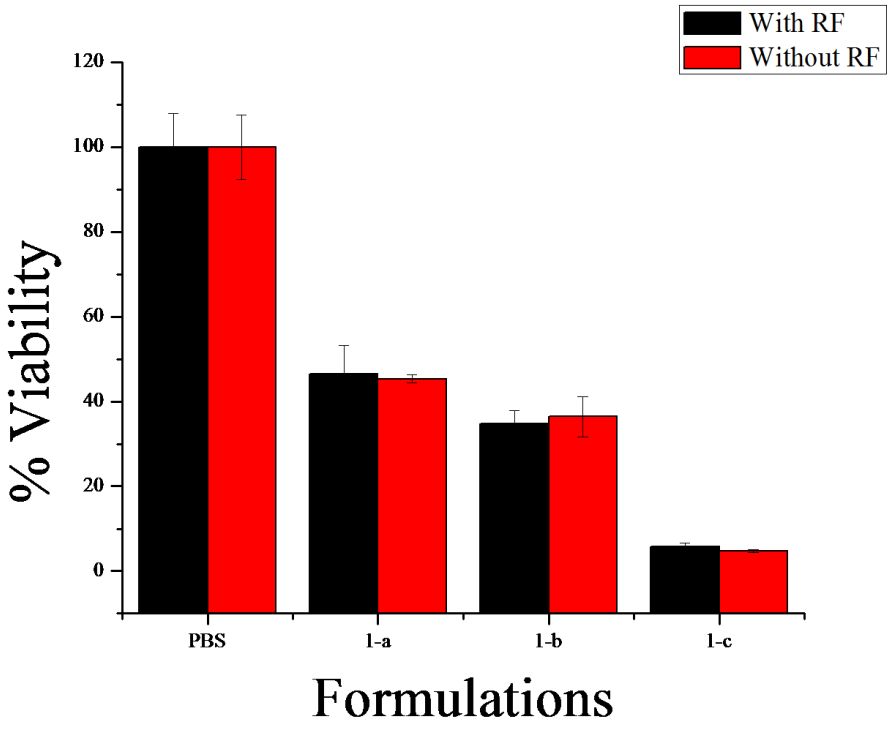

Figure 4. BxPC-3 cytotoxicity after 48 hours incubation and RF exposure at 4, 8, 20, 24, 28 and 40 hours for 30 minutes each. The incubated formulation contained 1) 0.5mM Gem + 0.5mM Cel + MNP (5000:1) with volumes of 20 µL (a), 50 µL (b) and 100 µL (c). (n=4, ± SD)

In order to overcome this issue, the same formulation was loaded with a lower MNP content (L/N ratio of 10,000: 1). As seen in Figure 5, a very less effect was seen with and without the application of RF heating. There was no statistically significant difference in the cell viability.

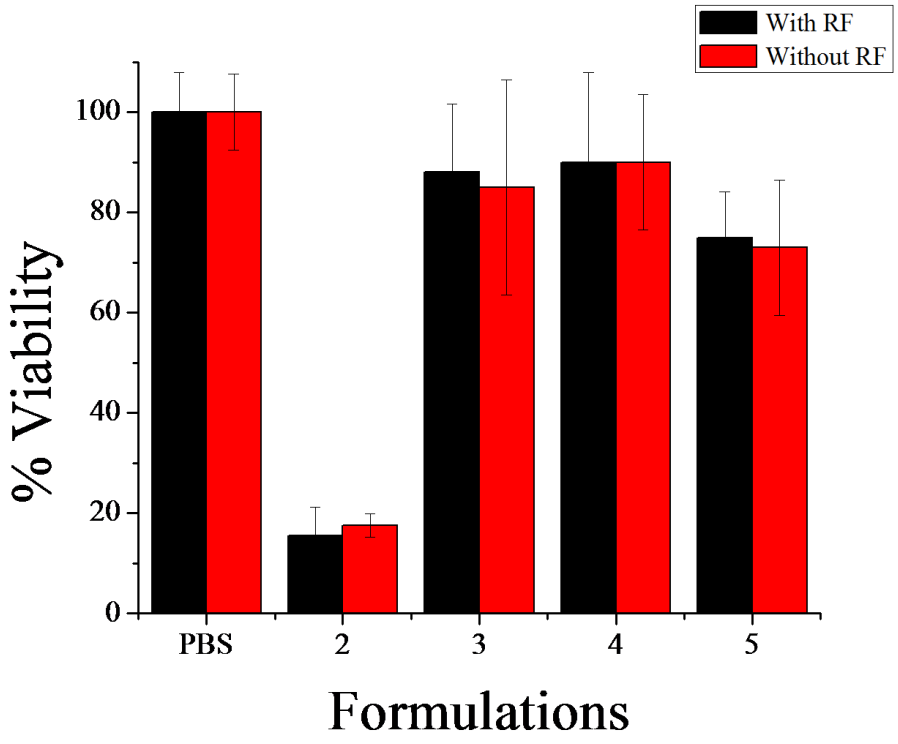

Figure 5. BxPC-3 cytotoxicity after 48 hours incubation and RF exposure at 4, 8, 20, 24, 28 and 40 hours for 30 minutes each. The incubated formulation contained:

2] 0.5 mM Gem + 0.5mM Cel + MNP (10000:1)

3] 5 µM Gem + 0.25 mM Cel +MNP (10000:1) - 17mM DPPC

4] 5 µM Gem + 0.25 mM Cel +MNP (10000:1) - 1:1 DPPC/DOPC wt/wt

5] 5 µM Gem + 0.25 mM Cel +MNP (10000:1) - 16mM DOPC

(n=4, ± SD)

In order to overcome the issue of concentration-driven drug diffusion from the vesicular bilayer, the GEM concentration was reduced to 5 µM while CEL concentration was kept at 0.5 mM as from our previous study it was seen that the hydrophobic drug RAL did not get released to a large extent from the bilayer despite of RF heating. Liposomes made of pure DPPC, 1:1 wt/wt of DPPC and 1,2-dioleoyl-

sn-glycero-3-phosphocholine (DOPC) lipid and pure DOPC were made for this experiment. As it can be seen from Figure 5 (5-3, 5-4 and 5-5), RF heating did not have a significant effect on the release of GEM or CEL (qualitatively determined by cell viability assay). The liposomes made from pure DOPC lipid showed maximum cell toxicity probably due to the unsaturated acyl chains that produce leaky liposomes. Finally, liposomes made with a reduced lipid concentration (10 mM DPPC) and low drug concentration of 5 µM GEM and 0.5 mM CEL were made with MNP (L/N ratio 10,000: 1). Three different volumes of formulations were incubated with the cells and similar studies were performed. It is evident form Figure 6 that the cell toxicity was the same with or without the application of RF heating.

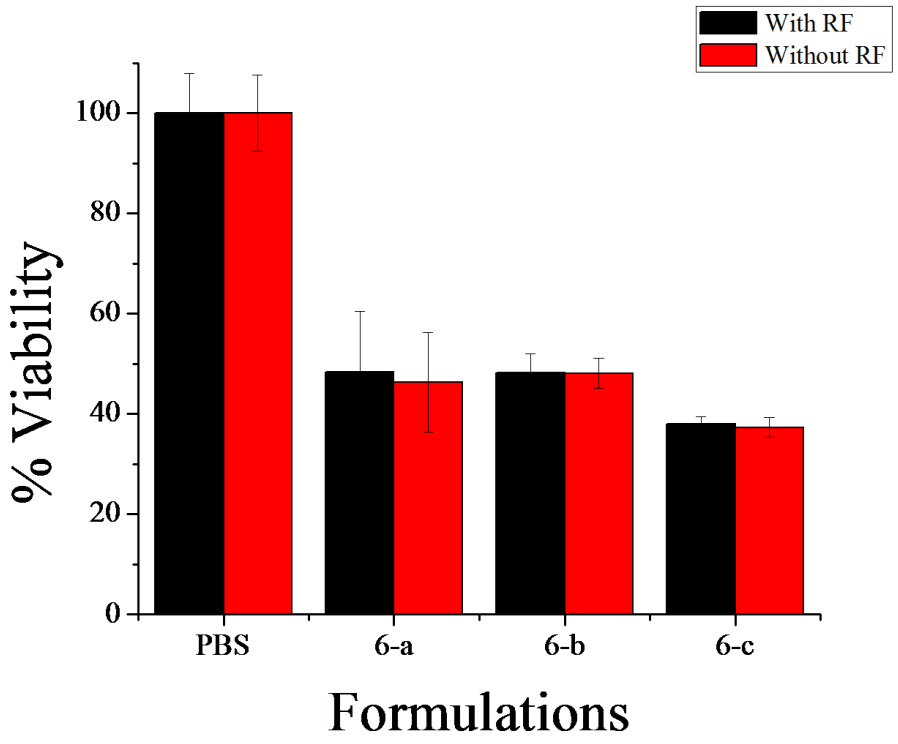

Figure 6. BxPC-3 cytotoxicity after 48 hours incubation and RF exposure at 4, 8, 20, 24, 28 and 40 hours for 30 minutes each. The incubated formulation contained 6) 5µM

Gem + 0.5mM Cel + MNP (10000:1) - 10mM DPPC with volumes of 20 µL (a), 50 µL (b) and 100 µL (c). (n=4, ± SD)

4. CONCLUSION.

It was observed that small hydrophilic molecule such as GEM was released from the liposomes containing CEL and MNP's irrespective of the application of magnetic field. This might be due to passive diffusion of GEM across the bilayer driven by a concentration gradient. Further study is necessary in order to optimize these liposomal formulations for better control of triggered release using magnetic field.

SUPPLEMENTAL INFORMATION.

1) **GEM calibration curve.**

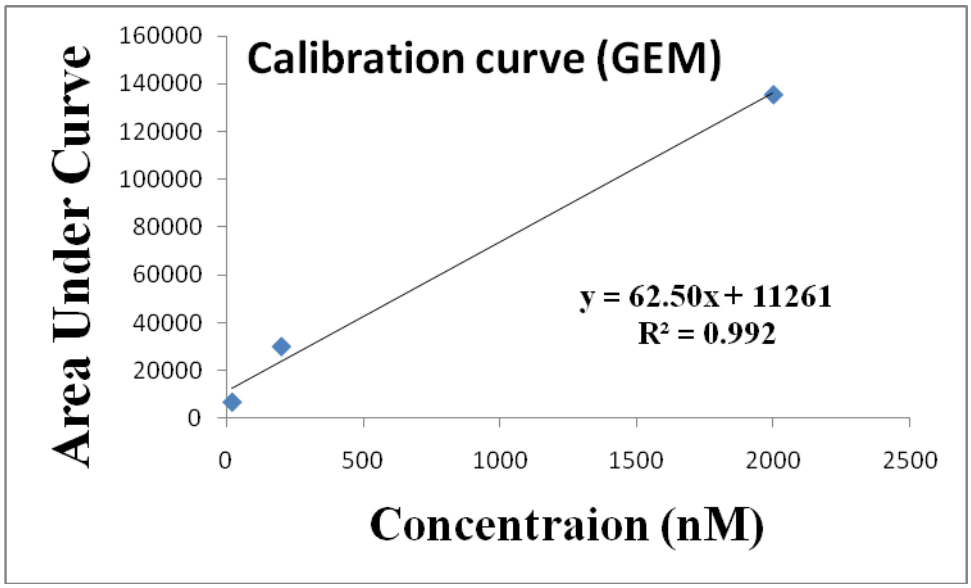

2) **HPLC chromatograms.**

a) **20 nM**

Area % Report

Data File: C:\EZChrom Elite\Enterprise\Projects\Default\Data\20nM_PBS_Gem4-2-20134-44-36 PMGemcetabine.met

Method: C:\EZChrom Elite\Enterprise\Projects\Default\Method\Swapnil\Gemcetabine.met

Acquired: 4/2/2013 4:45:48 PM

Printed: 4/3/2013 9:49:40 AM

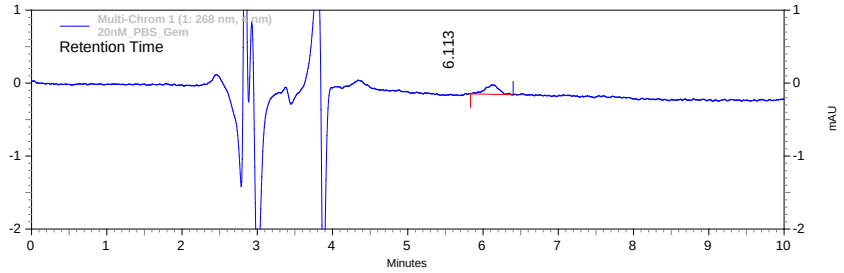

Chromatogram 1.

1: 268 nm, 4

nm Results

Retention Time	Area	Area %	Height	Height %
6.113	6776	100.00	512	100.00

Totals	6776	100.00	512	100.00

b) 200 nM

Area % Report

Data File: C:\EZChrom Elite\Enterprise\Projects\Default\Data\200 nM_PBS_Gem4-2-2013 4-55-53 PMGemcetabine.met

Method: C:\EZChrom Elite\Enterprise\Projects\Default\Method\Swapnil\Gemcetabine.met

Acquired: 4/2/2013 4:57:04 PM

Printed: 4/3/2013 9:48:34 AM

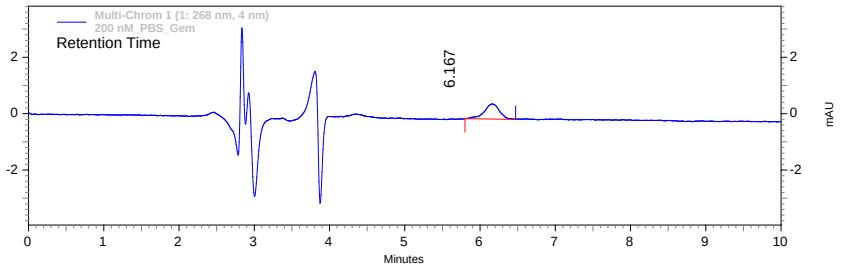

Chromatogram 2.

1: 268 nm, 4 nm

Results

Retention Time	Area	Area %	Height	Height %
6.167	30071	100.00	2138	100.00

Totals	30071	100.00	2138	100.00

c) 2000 nM

Area % Report

Data File: C:\EZChrom Elite\Enterprise\Projects\Default\Data\2000 nM_PBS_Gem4-2-2013 5-07-17 PMGemcetabine.met

Method: C:\EZChrom Elite\Enterprise\Projects\Default\Method\Swapnil\Gemcetabine.met

Acquired: 4/2/2013 5:08:28 PM

Printed: 4/3/2013 9:46:15 AM

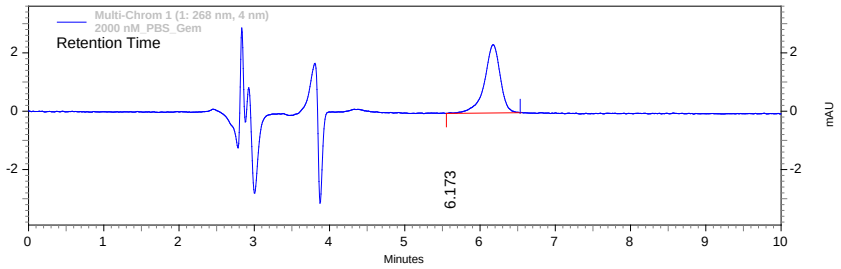

Chromatogram 3.

1: 268 nm, 4

nm Results

Retention Time	Area	Area %	Height	Height %
6.173	135703	100.00	9356	100.00

Totals	135703	100.00	9356	100.00

3) CEL calibration curve

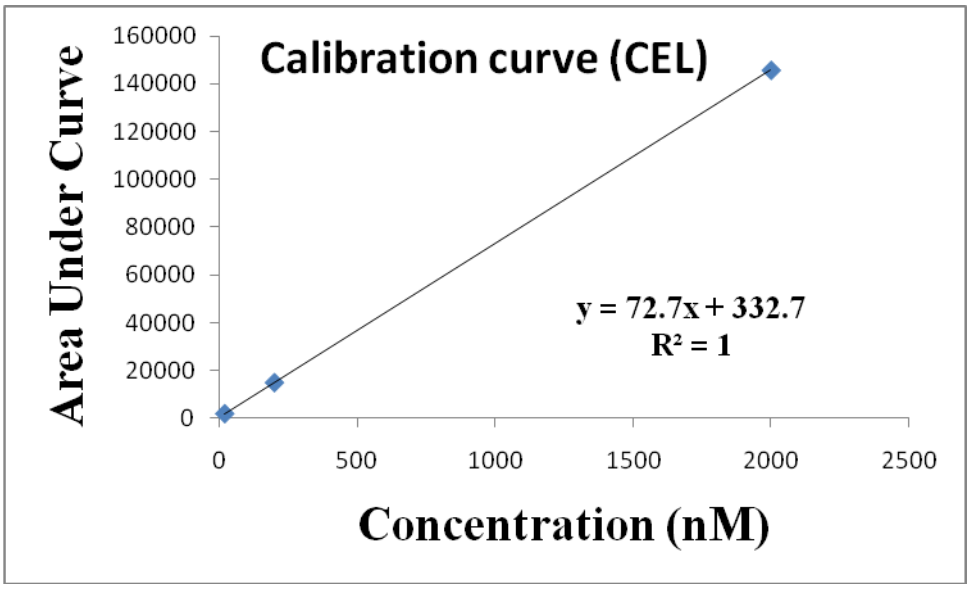

4) HPLC chromatograms.

a) 20 nM

Area % Report

Data File: C:\EZChrom Elite\Enterprise\Projects\Default\Data\Swapnil\Celecoxib\20nM_PBS_2Cel4-2-2013 3-35-11 PMCelecoxib.met

Method: C:\EZChrom Elite\Enterprise\Projects\Default\Method\Swapnil\Celecoxib.met

Acquired: 4/2/2013 3:36:23 PM

Printed: 4/2/2013 4:42:06 PM

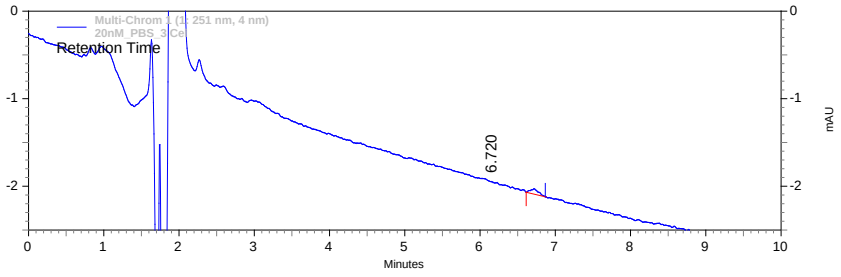

Chromatogram 1.

1: 251 nm, 4 nm Results

Area	Area %	Height	Height %

Retention Time				
6.720	1821	100.00	244	100.00

Totals	1821	100.00	244	100.00

b) 200 nM

Area % Report

Data File: C:\EZChrom Elite\Enterprise\Projects\Default\Data\Swapnil\Celecoxib\200 nM_PBS_2 Cel4-2-2013 3-46-34 PMCelecoxib.met

Method: C:\EZChrom Elite\Enterprise\Projects\Default\Method\Swapnil\Celecoxib.met

Acquired: 4/2/2013 3:47:45 PM

Printed: 4/2/2013 4:43:25 PM

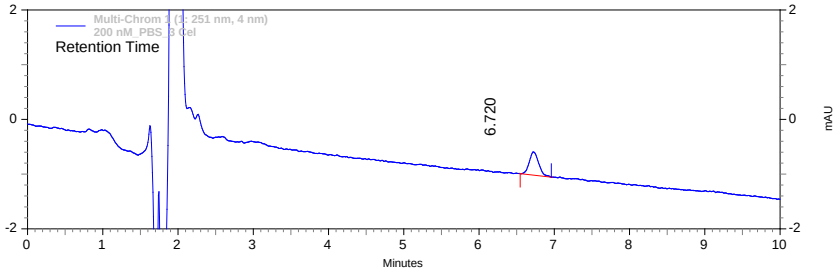

Chromatogram 2.

1: 251 nm, 4

nm Results

Retention Time	Area	Area %	Height	Height %
6.720	14835	100.00	1697	100.00

Totals	14835	100.00	1697	100.00

c) 2000 nM

Area % Report

Data File: C:\EZChrom Elite\Enterprise\Projects\Default\Data\Swapnil\Celecoxib\2000 nM_PBS_2 Cel4-2-2013 3-57-51 PMCelecoxib.met

Method: C:\EZChrom Elite\Enterprise\Projects\Default\Method\Swapnil\Celecoxib.met

Acquired: 4/2/2013 3:59:01 PM

Printed: 4/2/2013 4:44:44 PM

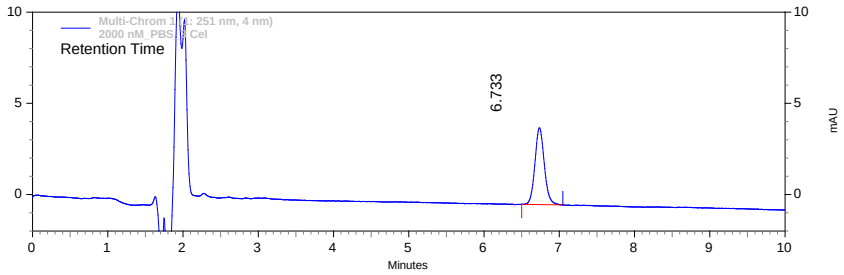

Chromatogram 3.

1: 251 nm, 4

nm Results

Retention Time	Area	Area %	Height	Height %
6.733	145736	100.00	16811	100.00

Totals				
	145736	100.00	16811	100.00

5. REFERENCES.

1. Siegel, R.; Ma, J.; Zou, Z.; Jemal, A. *CA Cancer J Clin* **2014,** 64, (1), 9-29.

2. Harris, A. L. *Nat Rev Cancer* **2002,** 2, (1), 38-47.

3. Maxwell, P. H. *Semin Cell Dev Biol* **2005,** 16, (4-5), 523-30.

4. Kullmann, F.; Hollerbach, S.; Dollinger, M. M.; Harder, J.; Fuchs, M.; Messmann, H.; Trojan, J.; Gabele, E.; Hinke, A.; Hollerbach, C.; Endlicher, E. *Br J Cancer* **2009,** 100, (7), 1032-6.

5. Herrmann, R.; Bodoky, G.; Ruhstaller, T.; Glimelius, B.; Bajetta, E.; Schuller, J.; Saletti, P.; Bauer, J.; Figer, A.; Pestalozzi, B.; Kohne, C. H.; Mingrone, W.; Stemmer, S. M.; Tamas, K.; Kornek, G. V.; Koeberle, D.; Cina, S.; Bernhard, J.; Dietrich, D.; Scheithauer, W. *J Clin Oncol* **2007,** 25, (16), 2212-7.

6. Zheng, Y.; Cai, Z.; Wang, S.; Zhang, X.; Qian, J.; Hong, S.; Li, H.; Wang, M.; Yang, J.; Yi, Q. *Blood* **2009,** 114, (17), 3625-8.

7. Hamacher, R.; Schmid, R. M.; Saur, D.; Schneider, G. *Mol Cancer* **2008,** 7, 64.

8. Wang, W.; Abbruzzese, J. L.; Evans, D. B.; Larry, L.; Cleary, K. R.; Chiao, P. J. *Clin Cancer Res* **1999,** 5, (1), 119-27.

9. Ng, S. S. W.; Tsao, M. S.; Chow, S.; Hedley, D. W. *Cancer Res* **2000,** 60, (19), 5451-5.

10. Ohhashi, S.; Ohuchida, K.; Mizumoto, K.; Fujita, H.; Egami, T.; Yu, J.; Toma, H.; Sadatomi, S.; Nagai, E.; Tanaka, M. *Anticancer Res* **2008,** 28, (4B), 2205-12.

11. Gong, J.; Xie, J.; Bedolla, R.; Rivas, P.; Chakravarthy, D.; Freeman, J. W.; Reddick, R.; Kopetz, S.; Peterson, A.; Wang, H.; Fischer, S. M.; Kumar, A. P. *Clin Cancer Res* **2014**.

12. Kokawa, A.; Kondo, H.; Gotoda, T.; Ono, H.; Saito, D.; Nakadaira, S.; Kosuge, T.; Yoshida, S. *Cancer* **2001,** 91, (2), 333-8.

13. Koshiba, T.; Hosotani, R.; Miyamoto, Y.; Wada, M.; Lee, J. U.; Fujimoto, K.; Tsuji, S.; Nakajima, S.; Doi, R.; Imamura, M. *Int J Pancreatol* **1999,** 26, (2), 69-76.

14. Merati, K.; said Siadaty, M.; Andea, A.; Sarkar, F.; Ben-Josef, E.; Mohammad, R.; Philip, P.; Shields, A. F.; Vaitkevicius, V.; Grignon, D. J.; Adsay, N. V. *Am J Clin Oncol* **2001,** 24, (5), 447-52.

15. Okami, J.; Yamamoto, H.; Fujiwara, Y.; Tsujie, M.; Kondo, M.; Noura, S.; Oshima, S.; Nagano, H.; Dono, K.; Umeshita, K.; Ishikawa, O.; Sakon, M.; Matsuura, N.; Nakamori, S.; Monden, M. *Clin Cancer Res* **1999,** 5, (8), 2018-24.

16. Tucker, O. N.; Dannenberg, A. J.; Yang, E. K.; Zhang, F.; Teng, L.; Daly, J. M.; Soslow, R. A.; Masferrer, J. L.; Woerner, B. M.; Koki, A. T.; Fahey, T. J., 3rd. *Cancer Res* **1999,** 59, (5), 987-90.

17. Maitra, A.; Ashfaq, R.; Gunn, C. R.; Rahman, A.; Yeo, C. J.; Sohn, T. A.; Cameron, J. L.; Hruban, R. H.; Wilentz, R. E. *Am J Clin Pathol* **2002,** 118, (2), 194-201.

18. Xiong, H. Q.; Plunkett, W.; Wolff, R.; Du, M.; Lenzi, R.; Abbruzzese, J. L. *Cancer Chemother Pharmacol* **2005,** 55, (6), 559-64.

19. Ferrari, V.; Valcamonico, F.; Amoroso, V.; Simoncini, E.; Vassalli, L.; Marpicati, P.; Rangoni, G.; Grisanti, S.; Tiberio, G. A.; Nodari, F.; Strina, C.; Marini, G. *Cancer Chemother Pharmacol* **2006,** 57, (2), 185-90.

20. Xiong, H. Q. **2012**.

21. Zhang, S.; Da, L.; Yang, X.; Feng, D.; Yin, R.; Li, M.; Zhang, Z.; Jiang, F.; Xu, L. *Toxicol Lett* 225, (2), 201-7.

22. Das, M.; Jain, R.; Agrawal, A. K.; Thanki, K.; Jain, S. *Bioconjug Chem* **2014**.

23. Youl, M.; Hashem, S.; Brade, A.; Cummings, B.; Dawson, L. A.; Gallinger, S.; Hedley, D.; Jiang, H.; Kim, J.; Krzyzanowska, M. K.; Ringash, J.; Wong, R.; Brierley, J. *Clin Oncol (R Coll Radiol)* **2014**.

24. Markman, J. L.; Rekechenetskiy, A.; Holler, E.; Ljubimova, J. Y. *Adv Drug Deliv Rev* **2013,** 65, (13-14), 1866-79.

25. Ding, X.; Cai, K.; Luo, Z.; Li, J.; Hu, Y.; Shen, X. *Nanoscale* **2012,** 4, (20), 6289-92.

26. Oliveira, H.; Perez-Andres, E.; Thevenot, J.; Sandre, O.; Berra, E.; Lecommandoux, S. *J Control Release* **2013,** 169, (3), 165-70.

27. Schleich, N.; Sibret, P.; Danhier, P.; Ucakar, B.; Laurent, S.; Muller, R. N.; Jerome, C.; Gallez, B.; Preat, V.; Danhier, F. *Int J Pharm* **2013,** 447, (1-2), 94-101.

28. Jain, M.; Wu, N. M. *Journal of Membrane Biology* **1976,** 34, 157-201.

29. Cullis, P. R.; de Kruijff, B. *Biochim Biophys Acta* **1979,** 559, (4), 399-420.

30. **Amicangelo, W. R. L. a. J. C.** *Inorg. Chem.* **1998,** 37, (20), 5317-5323.